Silver Nanoparticles Inhibit the Binding and Replication of Dengue Virus

A thesis submitted in partial fulfillment

of the requirements for the degree of

Master of Science.

By

KELLEY J. WILLIAMS

B.S. Aerospace Engineering, Virginia Tech 2002
M.S. Management, Embry-Riddle Aeronautical University, 2007
M.S. Combating Weapons of Mass Destruction, Air Force Institute of Technology, 2015

2015

Wright State University

WRIGHT STATE UNIVERSITY

GRADUATE SCHOOL

March 30th, 2015

I HEREBY RECOMMEND THAT THE THESIS PREPARED UNDER MY SUPERVISION BY KELLEY J. WILLIAMS ENTITLED "SILVER NANOPARTICLES INHIBIT THE BINDING AND REPLICATION OF DENGUE VIRUS" BE ACCEPTED IN PARTIAL FULFILLMENT OF THE REQUIREMENTS FOR THE DEGREE OF MASTER OF SCIENCE.

Committee on Final Examination

Courtney E.W. Sulentic, Ph.D.
Professor of Pharmacology & Toxicology

Nancy J. Bigley, Ph.D.
Thesis Director
Professor of Microbiology and Immunology

Ioana Pavel-Sizemore, Ph.D.
Professor of Chemistry

Barbara Hull, Ph.D.
Director, Microbiology and Immunology

Robert E. W. Fyffe, Ph.D.
Vice President for Research and Dean of the Graduate School

ABSTRACT

Williams, Kelley J. M.S. Department of Microbiology and Immunology, Wright State University, 2015. Silver Nanoparticles Inhibit the Binding and Replication of Dengue Virus.

Dengue is an emerging hemorrhagic fever virus and widely considered the most important arbovirus in the world [1]. The CDC and the World Health Organization estimates Dengue virus (DENV) infects 50-400 million people annually in the tropical and subtropical regions of the world [2]. More than 500 thousand of these will develop severe infection and approximately 22 thousand will lead to death [3]. Dengue virus (DENV) is a positive-sense RNA virus that exists in 4 antigenic serotypes [4]. An immunological phenomenon called antibody-dependent enhancement (ADE) leaves a DENV victim vulnerable to increased risk of subsequent infections. Secondary infections with DENV are known to increase in severity from Dengue Fever (DF) to Dengue Hemorrhagic Fever (DHF) or Dengue Shock Syndrome (DSS). Currently, no vaccines or treatments are approved for DENV infections. Unsuccessful vaccine trials may open the door for non-traditional treatments such as silver nanoparticles. Silver nanoparticles (AgNP) are known to inhibit viral replication of numerous viruses but have never before been tested for inhibition of DENV. For the first time, this research presents reductions in DENV2 binding to Vero and RAW cells following pretreatment with AgNPs (6-10 nm, 8-25 μg/mL) and enhanced cell viability. These results suggest that similarly to other viruses, DENV infection can be inhibited at the first stage of the virus replication cycle, binding & entry.

HYPOTHESIS

Null Hypothesis: Silver nanoparticles do not inhibit the replication cycle of DENV serotype 2 (DENV2), inferred through statistically insignificant reduction in fluorescence intensity visualization and cell viability.

Alternate Hypothesis: Silver nanoparticles inhibit the replication cycle of DENV2, inferred through reduced fluorescence intensity visualization and enhanced cell viability.

TABLE OF CONTENTS

LIST OF FIGURES

Figure **Page**

LIST OF TABLES

Table **Page**

LIST OF ABBREVIATIONS

μg	microgram
μL	microliter
ADE	antibody-dependent enhancement
Ag	silver
AgNP	silver nanoparticle(s)
DLS	dynamic light scattering
DNA	deoxyribonucleic acid
FBS	fetal bovine serum
mg	milligram
mL	milliliter
MTT	3-(4,5-Dimethylthiazol-2-yl)-2,5-diphenyltetrazolium bromide
mV	millivolt
NHP	non-human primate
nm	nanometer
NP	nanoparticles
PBS	phosphate buffered saline
PdI	polydispersity index
PEG	polyethylene glycol
SD	standard deviation
ss(+)RNA	single-strand positive sense ribonucleic acid
SEM	scanning electron microscopy
TEM	transmission electron microscopy
UV-Vis	ultraviolet to visible absorption spectroscopy
Z-Ave	Z- average diameter

ACKNOWLEDGEMENTS

I would like to express my sincere appreciation to my faculty advisor, Dr. Nancy Bigley, and committee members Dr. Iona Pavel-Sizemore and Dr. Courtney Sulentic for their guidance and support throughout the course of this research. Your guidance and trust were certainly appreciated. I would, also, like to thank my wife and children for enduring my academic endeavors.

Great thanks are also due to Dr. Eric Vela, Arathi Paluri, Kevin Dorney, Erica Rinehart, and Nagarjuna Reddy Cheemarla, for their contributions and insight with this research.

Kelley J. Williams

INTRODUCTION

Dengue as a Global Threat

Dengue is a disease caused by four closely related viruses known as dengue virus -1 through -4 (DENV1-DENV4). DF is a disease that became prevalent in tropics during the great shipping industry expansion in the 18th and 19th centuries [5]. The principle arthropod vectors of dengue virus, the *Aedes aegypti* and *Aedes albopictus* mosquitoes, determine the geographic distribution of the disease. Approximately 40% of the world's population (2.5 billion people) live in a region at risk of dengue [2]. Dengue is typically spread throughout the tropical and subtropical latitudes, but has demonstrated the ability to spread to new areas, such as Europe, Croatia, the United States, and Portuguese islands [2]. Based on the morbidity of dengue infection and the widespread presence of its vectors, DENV is considered the most important arbovirus (arthropod-borne virus) in the world [1]–[3]. Vector control is the primary means of stopping an outbreak and ending the disease transmission cycle.

Dengue as an Emerging North American Threat

Dengue is endemic and a growing threat to the human population [3]. Although DF is uncommon among US citizens, it is a top priority for health and medical services in endemic areas.

Dengue is a historic problem within the continental United States. Between 1977 and 1987, 1655 suspected cases of dengue were observed in the southern states, 345 of which were confirmed by serological tests [4]. These cases occurred long after dengue was eliminated from the southern US in the 1920s. This example shows that the potential

for reintroduction of dengue still exists. The most recent outbreaks of DENV occurred in Hawaii (2001), Texas (2005), and Florida (2014) [3].

DENV is classified as a Biosafety Level 2 (BL-2) virus. Some fear that biological agents could be used to contaminate water supplies. DENV is not found naturally in water supplies and must infect living cells to replicate. Dengue is not lethal unless severe shock or other complications are involved. DENV is expected to survive in untreated water for short periods but not is not expected to survive common water treatment methods [6]. In this suspended form, DENV would not be infectious and requires parenteral transmission. Dengue is only infectious through parenteral transmission which greatly limits the potential for non-vector dissemination.

While DENV1-4 are in common circulation, DENV5 is suspected in a single outbreak in Malaysia. If confirmed, the a 5th DENV serotype presents challenges for the future of DENV vaccines and treatments [7]. Many scientists are skeptical about the serological independence of DENV5 and feel more research is necessary to determine if it is not a mutant of another DENV serotype or the result of sequencing error [20].

Dengue Pathology

DENV is transmitted through the bite of an infected female mosquito during its blood meal [8]. Humans are a dead-end host and the infection is not transmissible between humans. A noninfected *Aedes* mosquito can become infected through a blood meal on an infected human. After 4-10 days post-infection, a mosquito is an infectious vector for the remainder of its life [2]. The severity of an individual's infection depends largely on the history of infection and is characterized by the three clinical categories –

DF, DHF, or DSS. Primary infection may be asymptomatic or lead to classic dengue fever. Secondary infections may lead to the serious conditions of DHF or DSS [1].

The World Health Organization (WHO) estimates that 50-100 million people are infected with DENV each year. Due to the lack in accurate and timely reporting and the absence of adequate medical facilities in endemic regions, other sources, such as the Centers for Disease Control (CDC) place this estimate as high as 400 million annual infections [3]. Classic DF is the predominant syndrome. DHF accounts for over 500 thousand reported cases and there are over 22 thousand deaths annually [2].

Classic DF is also known as "breakbone fever", and was first described by Benjamin Rush during an outbreak in Philadelphia in 1780 [8]. DF begins after a 5-8 day incubation period with the abrupt onset of fever (103-106^{0}F) and headache (Figure 1). In the first day or two of fever, the face flushes and a generalized macular rash becomes evident. Between days 4-6, symptoms include nausea, vomiting, anorexia, and swollen lymph nodes (lymphadenopathy). The fever typically lasts 4-6 days and often culminates with a secondary maculopapular rash. The level of viremia generally coincides with fever.

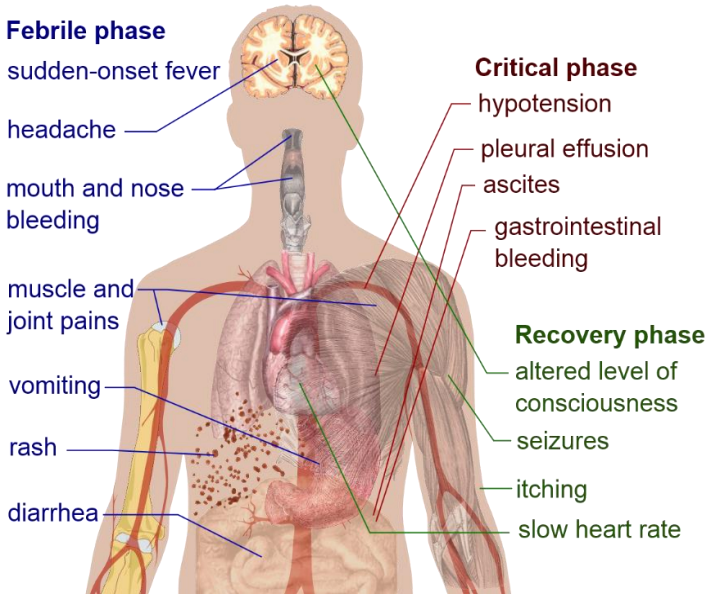

Figure 1. Symptoms of dengue fever. Public domain image, via Wikimedia Commons.

DHF and DSS are severe forms of dengue infection that can lead to death. DHF and DSS are common in areas with multiple endemic DENV serotypes. These serious illnesses begin with typical DF. Severe symptoms follow 2-5 days later with petechiae, bruising, and large spontaneous bruising (ecchymosis).

Table 1. World Health Organization grades of DF, DHF, or DSS [9].

Grade of disease	Disease type	Signs and Symptoms
I	DF	Fever accompanied by nonspecific constitutional symptoms with a positive tourniquet test as the only hemorrhagic manifestation
II	DHF	Same as grade I, except with spontaneous hemorrhagic manifestations
III	DSS	Circulatory failure manifested by rapid, weak pulse with narrowing of the pulse pressure (<20 mmHg) or hypotension
IV	DSS	Profound shock with undetectable blood pressure and pulse

Antibody-Dependent Enhancement

DHF and DSS are typically found in cases of secondary infection with a DENV serotype different from that of primary infection. These clinical developments are brought on by an immunological phenomenon called ADE. ADE can occur when someone is infected with any of the 4 DENV strains and then secondarily infected with another DENV strain. For example, following a successful adaptive immune response to primary DENV1 infection, antibodies are created which recognize DENV1 epitopes and can assist only in the neutralization DENV1. During a secondary infection with DENV2, the circulating antibodies that recognize DENV1 attach to the unfamiliar DENV2 particles and facilitate endocytosis by macrophages by means of the cognate (DENV-

recognizing) receptors. However, the circulating antibodies only weakly activate the cellular defenses and the virus will still undergo replication. Additionally, the DENV1 antibodies bound to DENV2 particles will be able to bind and enter cells through the Fc (constant) receptors which are ubiquitously expressed. This additional infectious pathway greatly contributes to the progressive symptoms of severe dengue (DHF/DSS).

Challenges to Dengue Therapeutics

The design and implementation of a dengue vaccine is complicated by numerous factors. First, the candidate vaccine must provide equal and lasting immune responses against all DENV serotypes. This requires a tetravalent vaccine to address DENV1-4. This vaccine would also need to solicit neutralizing antibodies regardless of the individuals existing immune status to DENV [9]. A second challenge is that there is no correlate of protection. Since the mechanism of DENV infection is not completely understood, the required antibody titers and impact of additional immunological pathways require further study [10]. Third, current animal models do not recapitulate both the disease outcome and a predictive immune response in humans with high levels of correlation. Currently, mouse and non-human primate (NHP) models are used to evaluate vaccine candidates. Mouse models for DENV are complicated often complicated by the inability of human clinical isolates to replicate well in mice, although the interferon receptor-deficient AG129 mouse model shows great promise [11], [12]. Some mouse models require modification of the viral genome to present clinical disease and may not be indicative of efficacy in humans. The NHP model does not present

clinical disease but does demonstrate viremia. Possibly due to these factors, discordance is occasionally observed between preclinical and clinical trials [13].

Vaccines development is complicated by small mutations in DENV serotypes. One common mechanism of each DENV serotype and flaviviruses in general is the action of RNA-dependent RNA polymerase (RdRp). This enzyme catalyzes the replication of RNA from the ss(+)RNA strand [14], [15]. Novartis developed an adenosine nucleoside inhibitor (NITD008) which directly inhibits the RdRp activity of DENV in vitro and in vivo. NIT008 is an adenosine analog with several substitutions; a carbon for N-7 of the purine and an acetylene at the 2' position of ribose [15]. Potential may exist for AgNPs to inhibit DENV by binding to exposed disulfide motifs within DENV RdRp [14].

Nanoparticles as an Antiviral Treatment

Nanoparticle therapeutics are in their infancy and there are currently no FDA approved nanotherapeutics [16]. Several studies demonstrate the systemic effects of silver nanoparticles through various routes of exposure [17]–[20]. In a mouse model, inhalational and gastrointestinal exposure (1-3 months) to AgNPs (20 nm, citrate stabilized) did not show severe systemic toxicity but intravenous exposure has potential to suppress the functional immune system in a dose-dependent manner (0.0082-6 mg/mL) [18]. Research also suggests that NP have potential to penetrate the blood-brain barrier (BBB) through intravenous and intraperitoneal exposure at high doses (25-100 mg/kg) [17].

These and similar studies offer unique insight to in vivo actions of AgNPs but they do not offer broad applicability outside the structure of the research. Published

research involving AgNPs does not consistently provide full characterization of the administered silver with respect to silver ion content, particle agglomeration, particle size distribution, surface coatings, or presence of synthesis byproducts. Since these additional factors play a critical role in AgNP biocompatibility and in vivo response, such omissions reduce the transferability of those data. Above certain concentrations (often >100 μg/mL), AgNPs may induce neurotoxicity by altering gene expression and generating free radical-induced oxidative stress [17]. The possibility that this effect is due to higher concentration of silver ions must be considered. This can lead to DNA damage, chromosomal aberrations, and cell death [21]. If AgNPs are to be utilized in clinical settings, the applied concentration must be well characterized under in vivo applications and remain under the cytotoxic levels.

LITERATURE REVIEW

Dengue Virus Summary

DENV is a member of the Flavivirus family, as is the yellow fever virus (the family's prototype), West Nile, Japanese encephalitis virus, and many others. DENV is also categorized as a Group IV ss(+)RNA virus under the Baltimore Classification. Based on serological studies, four serotypes of DENV (DENV1-4) are known to exist [22], [23]. These distinct serotypes present conserved structural and non-structural proteins although the genome identity between serotypes ranges from 23-73% [24], [25]. DENV virions exist in one of four stages of maturation. Only one of the four stages is infectious and considered mature. The mature virions exist in the extracellular environment while the three immature virion forms are primarily found intracellularly.

A mature DENV virion is composed of envelope proteins surrounding a nucleocapsid core which contains the viral genome. The genome consists of a single, positive-sense strand of RNA, approximately 10.7kb in length. The vRNA is translated into a single polyprotein. Viral and host proteases cleave this into three structural (C, prM, E) and seven non-structural (NS1-NS2A-NS2B-NS3-NS4A-NS4B-NS5) proteins [4]. The genome is surrounded by an icosahedral nucleocapsid C (capsid) protein approximately 30 nm in diameter [8]. The nucleocapsid is disordered and associated with the vRNA in an overlapping region [26]. This core is surrounded by a lipid bilayer then a well-organized icosahedral envelope which consists of E-prM protein heterodimeric complexes [8], [27].

DENV successfully grows in many cells lines from vertebrate and invertebrate hosts, but the most common are the C6/36 (ATCC® CRL-1660™) derived from the *Aedes albopictus* mosquito and the *Cercopithecus aethiops* (African green monkey) kidney epithelial (Vero) cell lineage [8], [28]. Selection of the C6/36 cells for DENV research is often preferable since they originate from the virus host. The titer of DENV isolated from C6/36 cell propagation tends to higher and express less mutations than isolates from Vero cells propagation [28]. However, as an invertebrate cell line, the utilization of C6/36 cells requires growth at 28^{o}C. Since this was a condition not supported at the researcher's laboratory facility, Vero cells were selected as a suitable cell line for virus propagation and additional assays.

Dengue Virus Binding and Entry

Dengue virus binds to mammalian cells through a wide range of cell-surface receptors and co-receptors [29]. Among the known DENV receptors, heparin sulfate (Vero cells), DC-SIGN, and the mannose receptor (macrophages) appear to play a critical role [30], [31]. In the event of antibody-dependent enhancement, the ubiquitous Fc receptor enhances DENV infection by binding anti-DENV antibodies and providing another entry pathway [32]. The DENV E protein (envelope glycoprotein) is the central epitope during binding. Once bound to the cell, DENV is trafficked in a diffusive manner along the cell surface until reaching a pre-existing clathrin-coated pit [33]. Dengue entry into mammalian cells may occur through multiple mechanisms, dominated by clathrin-mediated endocytosis and macropinocytosis [34], [35].

In the dominant case of clathrin-mediated endocytosis, DENV is internalized when the clathrin-coated pit invaginates and surrounds the particle. Now considered an endosome, the pH is lowered through action of proton pumps. The acidic pH causes a conformational change in the E protein below pH 6.2, causing it to become spiked in appearance [32]. The hydrophobic tips of the spiked envelope proteins penetrate and fuse with the endosomal membrane, releasing the DENV genome into the cytoplasm.

Silver Nanoparticles as Antiviral Agents

During the course of this research, the interaction of AgNPs with 10 virus species were identified (Table 2). Each study concluded that AgNPs inhibited virus replication under specific conditions. The mechanism of inhibition was not consistent among all viruses and some mechanisms are still unknown. One common conclusion was that

inhibitory mechanisms occurred early in the replication cycle, most commonly inhibiting the binding and entry of a virion into a host cell. Common experimental conditions which led to successful inhibition include:

- Antiviral activity dependence on AgNP size
- AgNP diameters between 8-25 nm
- AgNP concentrations between 8-50 µg/mL
- Tangential flow filtration (TFF) for AgNP size selection and silver ion removal
- AgNPs which are naked or capped or stabilized with citrate, polyethylene glycol (PEG), or polyvinylpyrrolidone (PVP)

I dsDNA	II ssDNA	III dsRNA	IV ss(+)RNA	V ss(-)RNA	VI ssRNA-RT	VII dsDNA-RT
Vaccinia [36] Monkeypox [37] HSV2 [38] Adenovirus			DENV	H1N1 [39] H3N2 [40] TCRV [41] RSV [42]	HIV-1 [43]–[46]	HBV [47]

Table 2. Existing research silver nanoparticles as antiviral treatments. Organized by Baltimore Classification.

Dengue Virus Type-2 (DENV2, New Guinea C strain)

Citrate stabilized AgNPs (10 nm) inhibited binding of DENV to Vero 76 cells at concentrations of 10 µg/mL and 25 µg/mL [48]. Based on indirect immunofluorescence analysis of anti-DENV E protein, incubation of AgNPs with DENV reduced fluorescence intensity by 92-96% (25 µg/mL and 10 µg/mL respectively). This evidence did not elucidate the mechanism of inhibition as being either antiviral (acting against the virions) or cytoprotective (binding to cell surface receptors and preventing virus binding). Additionally, this result was obtained in epithelial cells, demonstrating an off-target

effect of DENV infection. The targets of DENV infection in mammals are macrophages. It is necessary to examine the interaction of AgNP-DENV during the course of macrophage infection since this is a more natural condition. In this work, Vero cells were incubated with treatments (AgNP-DENV, DENV only, and AgNPs only) at 4^{o}C to permit binding but inhibit internalization of AgNPs and DENV. Based on immunofluorescence analysis, DENV (MOI 10) pretreated with AgNPs (10 µg/mL and 25 µg/mL), resulted in far fewer bound virion compared to DENV infection without

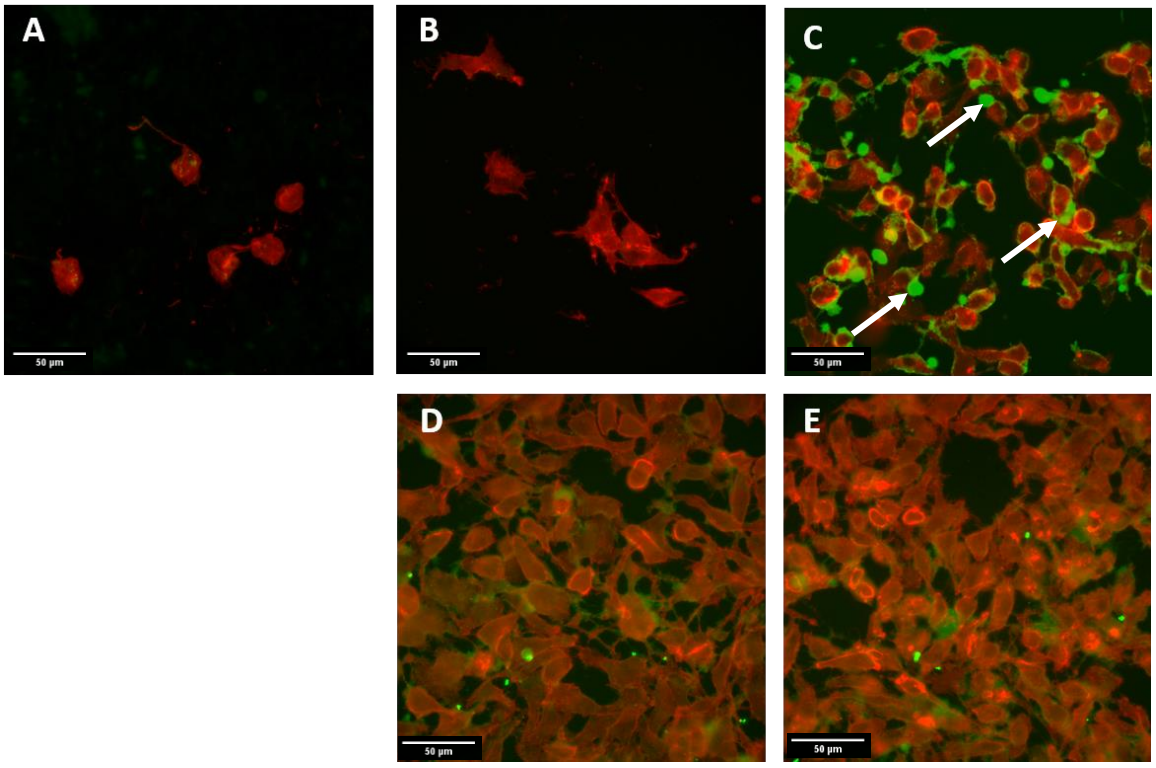

Figure 2. AgNP treatment blocks binding of DENV to Vero cells in 4^{o}C. A) mock-treated Vero, no AgNP or DENV B) isotype control, normal mouse IgG, no AgNP or DENV, C) DENV infection (white arrows) of Vero cells without AgNP treatment (MOI 10), D) DENV binding inhibited by pre-treatment with AgNP (25 µg/mL), E) AgNP treatment with Vero cells and no DENV (25 µg/mL). Green fluorescence (FITC, DENV E protein) and red fluorescence (TRITC, f-actin). Fluorescence images were captured at identical optical and processing software settings. Images enhanced +40% brightness, -40% contrast for better viewing in print. Scale bar: 50µm [48].

AgNP treatment (positive control) and negative controls (Figure 2). The reduction in FITC intensity was evaluated in Image J. Untreated DENV presents greater green fluorescence than after AgNP treatment (Figure 3). Compared to DENV-only,

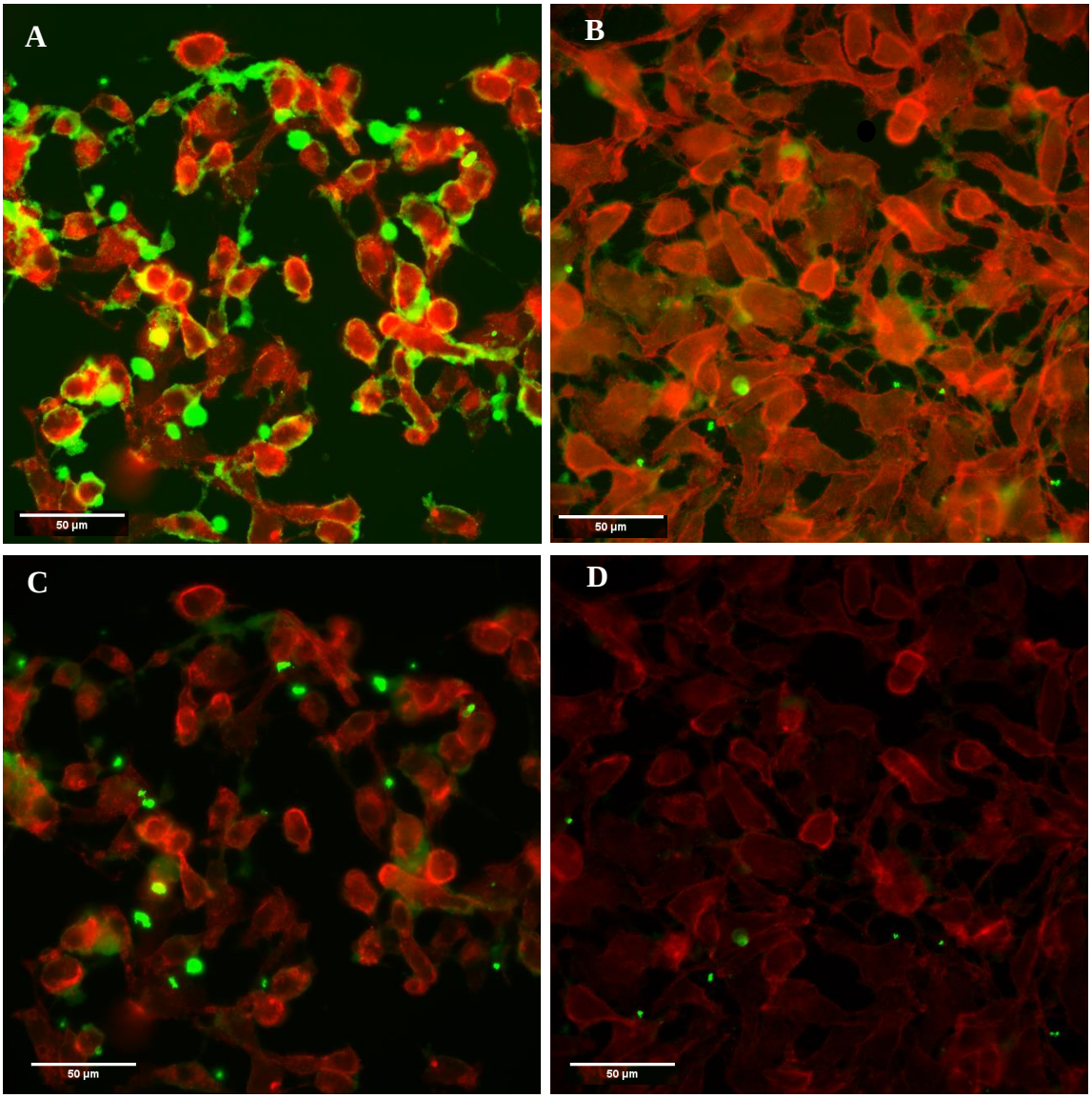

Figure 3. AgNP treatment blocks binding of DENV to Vero cells in 4°C. (A) DENV binding to Vero cells without AgNP treatment, (B) DENV binding inhibited by pre-treatment with AgNP (25 µg/mL). Green fluorescence (FITC, DENV E protein) and red fluorescence (TRITC, f-actin). Image brightness and contrast enhanced 40% for better viewing in print (A & B). (C & D) Non-enhanced composites. Scale bar: 50µm.

pretreatment with 10 µg/mL reduced DENV binding by a factor of 23.2. Pretreatment with 25 µg/mL reduced DENV binding by a factor of 12.2.

Interestingly, the higher concentration of AgNPs (25 µg/mL) resulted in approximately twice the fluorescence intensity of the lower concentration (10 µg/mL). One possible reason this occurred is that higher AgNP concentrations contributed to increased agglomeration. This could reduce the effective number of AgNPs available to bind with DENV particles and therefore lead to reduced DENV binding inhibition.

Comparison of the fluorescence histograms (normalized by cell count) revealed statistically significant differences ($P<0.001$, Mann-Whitney test) in the fluorescence intensity of treated cells and controls, and between the AgNP-treated DENV and DENV-only treatments.

While cold incubation does not reflect in vivo conditions during infection, this condition is effective when attempting to isolate the step at which AgNPs may inhibit the DENV life cycle. These results are similar to research showing AgNP inhibition of various viruses at the binding and entry phase of viral replication.

Vaccinia virus (VACV)

Silver Nanoparticles demonstrated cytoprotective and virucidal effects during VACV infection of Vero cells [36], [46]. Adsorption of VACV was not prevented when Vero cells were pretreated with AgNPs (11 nm, 8-128 µg/mL), as determined by plaque assay. The entry of vaccinia virus into Vero cells is inhibited by AgNPs at values above 48 µg/mL as determined by a β-gal (beta galactosidase) assay under the control of a constitutively active promoter. Through confocal microscopy quantification, VACV

entry was inhibited when pretreated $\geq$ 16 µg/mL. VACV is an enveloped dsDNA virus that replicated entirely in the cytoplasm. VACV is in the family Poxviridae and contains both a large genome (~190kbp) and large virion (~300 nm). VACV enters host cells through macropinocytosis and direct fusion.

Monkeypox virus (MPV)

MPV infection of Vero cells was inhibited by 10 nm polysaccharide-coated AgNPs [37]. AgNPs in diameters of 10-80 nm, concentrations from 12.5-100 µg/mL, and either polysaccharide coated or naked were tested against MPV in plaque reduction assays. Only the 10 nm PS-coated AgNPs reduced mean PFU below control ($P \leq 0.05$). This result is similar to HIV-1 studies with AgNPs where smaller particles (1-10 nm) provided the best antiviral activity. Rogers, et al. suggest the small particles effectively bind to viral epitopes and block the binding complex between virus and cell surface receptors and co-receptors. Another conclusion of this research was that the mechanism of inhibition is unknown but may "involve blocking of MPV to host cells, disruption of host cell biochemical pathways, or both" [37]. MPV is similar to VACV in size and replication cycle.

Herpes simplex virus (HSV)

AgNPs of unspecified diameter and concentration reportedly inhibit HBV2 in Vero cells. Sopova et al. described in the Russian journal (not translated to English) that "silver nanopowders" significantly reduced viral progeny in vitro. HSV is an enveloped dsDNA virus (152kbp) that enters host cells through fusion.

Adenovirus type 3 (ADV3)

Adenoviruses are non-enveloped dsDNA viruses with a diameter of 70–90 nm. ADV3 infection of HeLa cells was inhibited by AgNPs (11.4±6.2 nm) in concentrations from 3.125-50 µg/mL [49]. Cytopathic effects were observed in in HeLa cells when AgNP concentrations exceeded 50 µg/mL as seen in similar experiments. Unlike most AgNP antiviral experiments which treat cells and virus for 1 hour, Chen et al. treated for 2 hours. ADV3 that was treated with 50 µg/mL AgNPs for 30 minutes experienced conformational changes in the virion structure. Treatment for 90 and 120 minutes created dramatic damage to the virion. Unfortunately, the researchers did not mention whether their AgNP colloid contained significant levels of silver ions, the most likely cause of ADV3 damage.

Influenza A (H1N1 and H3N2 IFV)

H1N1 and H3N2 influenza A infection of Madin-Darby Canine Kidney epithelial (MDCK) cells was inhibited by non-coated AgNPs [39], [40]. AgNPs in these studies were characterized in the range of 5-120 nm (10 nm mean). This study found that when H1N1 or H3N2 IFV were pretreated for 2 hours with AgNP concentrations of 12.5-50 µg/mL, the viability of MDCK cells was significantly increased ($P<0.01$). When virus was incubated with AgNPs (50 µg/mL) for 30-120 minutes, the IFV experienced structural damage. Damage was observed even when there did not appear to be AgNPs bound to virions, indicating damage through silver ions. These studies recognized the potential significance of silver ions in an antiviral mechanism but did not present data on ion content in their colloid or any methods used to remove silver ions during experimentation.

Tacaribe virus (TCRV)

Tacaribe virus infection of Vero cells was inhibited by AgNPs of varying size and coating [41]. AgNPs (10 nm and 25 nm) that were either naked or polysaccharide-coated significantly inhibited viral progeny ($P<0.05$). AgNP concentrations above 50 µg/mL were determined to exhibit cytopathic effect. Unlike other AgNP antiviral studies, TCRV experienced enhanced uptake into Vero cells when in complex with 10 nm non-coated AgNPs (50 µg/mL). Replication was inhibited after entry to the cell by an unknown mechanism.

Respiratory syncytial virus (RSV)

RSV infection of HEp-2 cells was reduced by 44% after RSV pretreatment with poly(N-vinyl-2-pyrrolidone) (PVP) coated AgNPs [42]. These functionalized AgNPs exhibited low cytotoxicity at low concentrations.

Human immunodeficiency virus (HIV-1)

Several studies have determined that HIV-1 (or HIV-1 pseudotyped virus [46]) binding and entry to host cells can be inhibited by AgNP pretreatment [43]–[46]. Common conclusions indicate that AgNPs ($\leq$25 nm) bind to the glycoprotein 120 (gp120) knobs of the HIV-1 envelope but a 1-10 nm diameter is optimal [45]. This binding event blocks the formation of the gp120-CD4 complex and inhibits cell fusion. One study determined that the use of AgNPs and neutralizing antibodies had an additive inhibitory effect against cell-associated HIV-1 [44].

Hepatitis B (HBV)

AgNPs (10 nm & 50 nm, uncoated) inhibit hepatitis B virus replication in HepAD38 cells [47]. The suggested mechanism of inhibition is the direct interaction between AgNPs and the HBV dsDNA or virion. Lu et al. determined through TEM that the 10 nm particles were able to bind directly to the HBV virion. AgNPs had little effect on HBV circular DNA but inhibited the formation of HBV intracellular RNA. HBV is an enveloped dsDNA virus with a reverse transcription intermediate (dsDNA-RT). HBV is generally spherical and 42 nm in diameter (similar to DENV, 50 nm) but pleomorphic forms exist including filamentous and spheres without a nucleocapsid core.

Silver Ions

It is important for AgNP research to differentiate between effects of silver nanoparticles and silver ions. AgNPs are widely viewed as antimicrobial, but it may actually be the silver ions present in the colloid that impart protective effects. Silver ions (Ag^{+}) are known to possess antibacterial effects by the mechanism is not fully understood. Silver ions are also cytotoxic at much lower concentrations than ion-free AgNP colloids. Potential in-vivo treatments must utilize well-characterized silver colloids to ensure ion levels are safe. Silver ions interact with thiol groups in enzymes and proteins, altering their intended conformation and function [50]. Ions released from silver nanoparticle colloids is known to inactivate enterobacter aerogenes-specific bacteriophage (UZ1). Silver ions in the form of silver nitrate ($AgNO_3$) also inactivated the MS2 and T2 phages and implicated in the inactivation of numerous other viruses [37], [51], [52]. The bactericidal effect of silver ions are well known and provide the

antibacterial properties of silver used in medical dressings, surgical tools, and many commercial products [53].

Silver Nanoparticle Selection

Increasing attention for the potential of AgNP antiviral properties led to numerous studies regarding the influence of AgNPs' size, concentration, surface modification, and morphology on their viralcidal or cytoprotective effects [37]–[46]. Several reports indicate that uncoated, spherical AgNPs of approximately 10-20 nm in diameter are the most effective at preventing viral infection in a variety of cell lines while avoiding significant host cell cytotoxicity [37], [41], [45]. Such particles commonly exhibit non-cytotoxic antiviral effects at concentrations $\leq$50 μg/mL.

The Creighton synthesis is one of several methods available to produce spherical, uncoated AgNPs. The Creighton synthesis of AgNPs involves the reduction of silver nitrate (AgNO3) with sodium borohydride (NaBH4) in an aqueous matrix. This synthetic process results in a colloid containing spherical AgNPs of 1-100 nm in diameter. This method also results in trace amounts of non-reduced silver ions following the formation of AgNPs. Silver ions are known for their toxicity, providing the antibacterial properties of silver that is used in medical dressings, surgical tools, and many commercial products [53]. The resulting Creighton AgNPs are well characterized and have previously been utilized to investigate the AgNP antiviral mechanism against a common poxvirus (Pavel et al, pending publication).

MATERIALS AND METHODS

Overview

Research was conducted in three phases: characterization, fluorescence, and analysis. First, the key components of the research were characterized (Vero cells, AgNP, and DENV2). Vero cells were passaged 6 times to ensure they were free of foreign contamination and their growth curve was determined at 24 hour intervals. The silver nanoparticles used in this research were analyzed for size distribution, purity, concentration, and aggregation. DENV2 was propagated in Vero cells and titrated by plaque assay and flow cytometry. Second, the effect of AgNPs, DENV, and DENV-AgNPs were explored through immunofluorescence binding assays. The impact of AgNPs on DENV binding to Vero cells constituted the endpoint assay of this research. Third, the fluorescent images were processed and analyzed to determine the effect of AgNPs on DENV binding to Vero cells.

RAW 264.7 Cells

RAW 264.7 (ATCC® TIB-71™) cells are an adherent macrophage-like cell line derived from tumors induced in male BALB/c mice by the Abelson murine leukemia virus [54]. RAW cells present numerous cell surface receptors and co-receptors known and suspected to be involved in the binding of DENV, mainly the mannose receptor (CD206) and clathrin proteins.

Vero Cells

Vero 76 cells (CRL-1587, ATCC) are African green monkey kidney epithelial cells. Vero cells are commonly used in microbiology, molecular and cell biology research when a continuous mammalian cell line is required [55]. Vero cells are anchorage-dependent and susceptible to a wide range of viral infection, thus permitting the study of viral infection through plaque reduction assays and other common analytical techniques [55]. Vero cells have been used extensively with DENV and are a proven model for DENV experimentation [8], [28], [56].

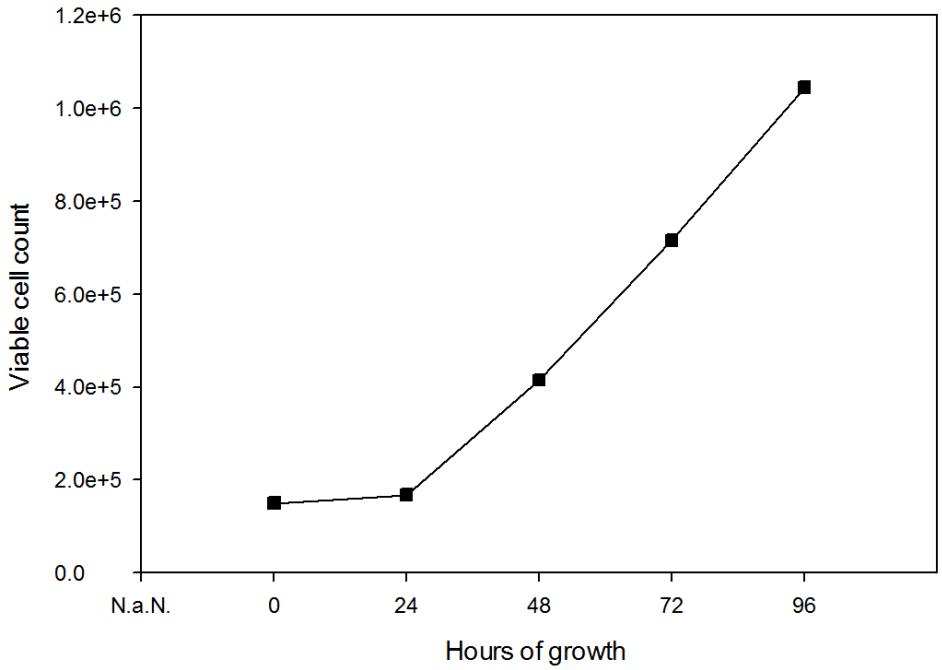

Figure 4. Vero cell 96-hour growth curve

To reliably perform experiments in cell culture with repeatable results, it is important to accurately predict the cell population at various points. Vero cell growth is commonly reported to double in each 24h period until day 6, when the growth is significantly slower [57]. Five 60mm petri dishes were seeded with Vero cells at a

density of $1.5x10^5$ per dish, as determined by the hemacytometer method of cell counting. At 24 hour intervals, one culture was removed from incubation and processed for cell counting as described below. Growth rates over 96h exhibited a 24h stabilization period and 80% growth every 24h period over 96h (Figure 4) as determined by cell counting using the hemacytometer method (described below). This curve established as a baseline for experiments influencing cellular growth rates and to provide greater consistency and predictability when preparing for experiments. The 96h timepoint was selected because many of the experiments in this research utilized a 96h window for DENV replication.

Cell Line Maintenance

RAW 264.7 (ATCC® TIB71™) and Vero 76 (ATCC® CRL-1587™) cells were maintained according to established protocols [54], [55]. Cells were maintained in DMEM/High Glucose (HyClone®) supplemented with 10% heat-inactivated Fetal Bovine Serum and 1% Penicillin/Streptomycin (Sigma®, 10k U/mL penicillin and 10 mg/mL streptomycin in 0.9% NaCl). During subculture procedures, cell count and viability was performed by the Trypan Blue exclusion test using a hemacytometer, described below. This permitted a high consistency in cell growth timelines and cell survival.

Virus Propagation

Propagation of Dengue virus serotype 2 (DENV2-NGC, donated by Dr. Eric M. Vela, Battelle Research Center) was performed in Vero 76 cells. The titer of virus stock was approximately $5.5x10^5$ PFU/mL upon receipt. Vero 76 cells were seeded at $1x10^6$ in 100 mm petri dishes in DMEM/High Glucose (HyClone®) supplemented with 10% heat-

inactivated Fetal Bovine Serum and 1% Penicillin/Streptomycin (Sigma®, 10k U/mL penicillin and 10mg/mL streptomycin in 0.9% NaCl). The cells were incubated at 37ºC and 5% CO_2 until they reached a confluency of approximately 90% then infected with DENV2 for 5 days, which was prior to significant cytopathic effects as observed through a light microscope. Previous research has demonstrated that the presence of serum in the growth media during DENV propagation does not inhibit the titer yield but is necessary for proper cell maintenance in culture [58]. The cells were then detached from the growth surface with Trypsin and centrifuged at 3200 rpm (2136x g) at 4ºC for 10 minutes to eliminate cell debris. Immature (non-infectious) isoforms of DENV are primarily intracellular and captured in the pellet following centrifugation. The intercellular virus recovered from the supernatant contains primarily mature (infectious) DENV although the various isoforms can never be isolated with 100% efficiency. The supernatant was aliquoted and stored at −80°C until use. Virus stock was filtered before use using 0.22μm filter membranes (EMD Millipore).

Silver Nanoparticle Synthesis and Filtration

Silver nanoparticles were synthesized using the Creighton method, described by Pavel et.al [59]. Tangential flow filtration (TFF) was employed to size-select AgNPs for viral inhibition studies. Typically reserved for biological separations, TFF operates on the continuous recirculation of a solution containing an analyte of interest across a porous membrane. As a solution or colloid is passed over the membrane, larger components are retained by the filter membrane and kept within the recirculation tubing while

constituents smaller than the filter pores are passed through the membrane and collected in a dilute filtrate.

By employing filters of varying pore size, AgNPs were size-selected for diameters of approximately 5-20 nm (6-10 nm average) and concentrated by removing excess solvent using membranes with ultrafine pore sizes (e.g., 5 nm in diameter). The TFF process resulted in a significantly concentrated colloid (i.e., 10 mL of AgNPs at a concentration of 1,000 μg/mL or higher) that can be utilized to create viral inhibition titers free of excess reagents, which might interfere with the interpretation of the antiviral mechanism exhibited by AgNPs. The concentration of nanosilver in the AgNP titers and TFF-obtained colloid was determined spectrophotometrically using inductively coupled plasma optical emission spectroscopy (ICP-OES).

Characterization of Silver Nanoparticles

AgNP characteristics monitored in this research include, size and size distribution, colloid concentration, zeta potential, and silver ion content. Characterization of nanoparticles was conducted at Dr. Pavel's facility, Wright State University. Following synthesis and prior to use, nanoparticles were characterized using the following work flow (Figure 5):

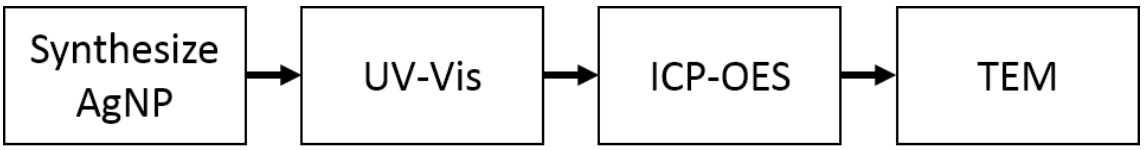

Figure 5. Work flow for AgNP characterization

- UV-Vis – Ultraviolet–visible spectroscopy (size/agglomeration)

- ICP-OES – Inductively coupled plasma optical emission spectrometry (concentration)
- TEM – Transmission electron microscopy (visualization, size).

AgNP-DENV2 Treatment

Silver nanoparticles were incubated with DENV2 at room temperature in various concentrations for one hour prior to Vero cell infection. This pre-treatment timeline was chosen in order to allow stable binding between DENV and the AgNP. Excessive incubation times were avoided because they could include effects of silver ions and bias the results.

Transmission Electron Microscopy (TEM)

TEM imaging of AgNP-DENV interaction was performed on a Hitachi H-7600 through cooperation with the University of Dayton's NEST Laboratory. This instrument has accelerating voltages of 40-120kV and a magnification range of 700x-600,000x which provides resolution of approximately 2 nm. This permits high resolution imaging of AgNPs and DENV particles. Preparing samples for TEM imaging was accomplished through fixation and osmium tetroxide (OsO_4) contrast staining.

Samples of AgNPs and DENV were co-incubated for one hour then fixed with 4% paraformaldehyde for 1 hour at room temperature. Samples were then stained with 1% (diluted in PBS) for 1 hour at room temperature in a chemical fume hood. A drop of the colloid was placed on a Formvar grid and air-dried. Representative images were taken at 30kx, 60kx, and 120kx.

Trypan Blue Exclusion Test (Hemacytometer method)

Trypan Blue staining was performed during cell culture to ensure continued viability of cells between passages. Trypan Blue staining was also performed to support the results of MTT assays (cell viability). After centrifugation, cells were suspended in DMEM and titurated thoroughly. A hemacytometer was cleaned with 70% ethanol and a 20mm glass coverslip was placed over the viewing grid. 50 µL of the cell suspension was added to 100 µL Trypan Blue stain in a 0.5 mL centrifuge tube and titurated thoroughly. This 50:100 ratio provided a dilution factor of 3. The cell-stain mixture was pipetted into the loading channel until the viewing grid was full (approximately 10 µL). Viable cells exclude the stain and appear white while dead cells take up the stain and appear blue. Eight grids were counted (living/dead) to provide cell viability as a percentage of total cells (Figure 6). Estimated cell count was determined by the formula:

$$\frac{Viable\ cells}{mL} = \frac{\#\ viable\ cells}{\#\ grids\ counted} * dilution\ factor * 10^4$$

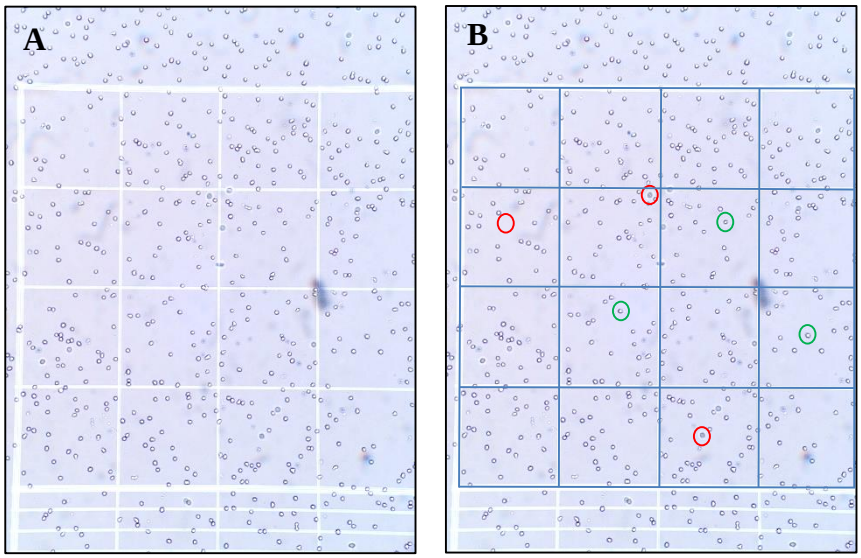

Figure 6. Trypan exclusion of RAW cells. A) Image a single 16-section grid from light microscope, B) Enhanced image with outlined sections and representative viable cells (green circles) and dead cells (red circles). Eight similar 16-section grids were counted during cell subculture and cell viability experiments.

MTT Assay

In addition to Trypan Blue exclusion, experiments involving the quantification of cell viability were conducted by MTT assay. MTT assays measure the reduction of 3-(4,5-Dimethylthiazol-2-yl)-2,5-diphenyltetrazolium bromide in viable cells by action of mitochondrial reductase to a purple formazan crystal. MTT assays (MarkerGene Technologies, Inc., M1475) were carried out in 96-well plates, with each experimental condition repeated 6-fold. Wells around the perimeter of the 96-well plate were not used due to increased risk of evaporation and greater variability experienced in those wells [60]. Once cells were prepared according to the particular experiment, treatments were removed and the cells were washed in 1% PBS. Next, 30 µL MTT (2 mg/mL) and 170 µL HEPES buffer (10 mM, pH 7.4) was added to each well and the cells were incubated for 3 hours at 37^{o}C and 5% CO_2. Following incubation and visual confirmation of the

formation of purple formazan crystals in mock treated wells, the MTT/HEPES solution was carefully aspirated and the crystals were solubilized with 100 µL dimethyl sulfoxide. After 15 minutes, the absorbance of each well was read at 570 nm (Figure 7) with a background of 620 nm in a spectrophotometer with 3 reads per well following 30 seconds of slow orbital rotation and 10 seconds of settling time. Quantitative results are averages of four measurements under the same conditions.

Biocompatibility of AgNPs in Vero cells

The biocompatibility of silver nanoparticles versus silver ions were determined through MTT assay. Vero cells were seeded at $2x10^4$ cells/well in a 96-well plate in DMEM-10 and incubated at 37°C and 5% CO_2. The cells were allowed to stabilize for 24 hours under these conditions prior to treatment. After 24 hours, the cells were exposed to

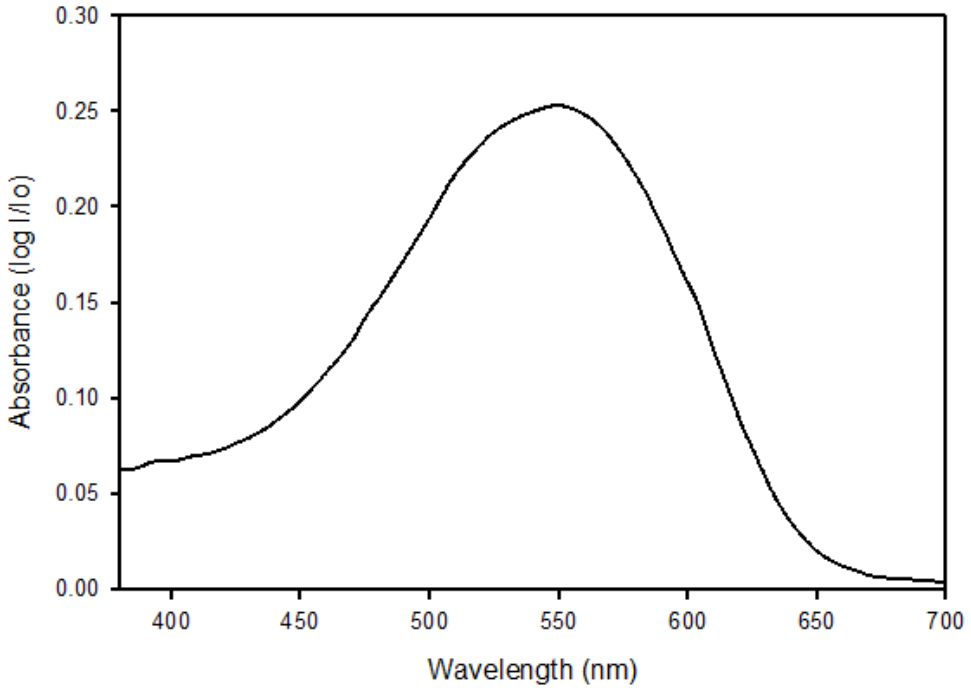

Figure 7. Absorbance spectrum of formazan in dimethyl sulfoxide

AgNPs or silver nitrate ($AgNO_3$) in concentrations of 100 µg/mL, 50 µg/mL, and 10 µg/mL, for 24 hours. MTT assay was performed as described above.

Infection with DENV Progeny Following Exposure to AgNP

The influence of AgNPs on the production of viral progeny was analyzed as related to Vero cell viability. Untreated DENV and DENV pretreated for 1 hour with 10 µg/mL or 25 µg/mL AgNPs (6-10 nm Creighton) were incubated with Vero cells (70% confluent) for 1 hour. Vero cells without DENV or AgNP treatment served as a mock control. Treatments were removed and Vero cells were washed three times with PBS to remove unbound DENV or AgNP. Cells received fresh DMEM and were incubated for 3 days, before significant cytopathic effects were seen in infected cells. Cells were trypsinized, centrifuged at 500 g, supernatant was collected by pipetting, and the cell pellet was suspended in DMEM. Cell pellets were counted by the hemacytometer method and compared to mock treated cells. Intercellular mature virions were concentrated using 100 kD centrifugal filters. Retained virions were suspended in DMEM-10 and filtered through a 0.22 µm vacuum filter to remove residual Vero cells, bacteria, or fungal contamination. This concentrated viral progeny was used to infect a second round of Vero cells (no new AgNP), grown to 70% confluency. Mock treated cells received only DMEM. Following 3 days of second round growth, cells were counted and compared to the mock treated control using a One-way ANOVA.

AgNP Influence on RAW Cell Viability during DENV Infection

To determine the influence of AgNP treatment during DENV infection on RAW cell viability: Untreated DENV and DENV pretreated for 1 hour with 10 µg/mL or 25

μg/mL AgNPs (6-10 nm Creighton) were incubated with RAW cells (50% confluent) for 1 hour. RAW cells without DENV or AgNP treatment served as a mock control. Treatments were removed and RAW cells were washed three times with PBS to remove unbound DENV or AgNP. Cells received fresh DMEM and were incubated for 3 days, before significant cytopathic effects were seen. Cells were trypsinized, centrifuged at 500g, the supernatant collected, and the cell pellet was suspended in DMEM. Cell pellets were counted by the hemacytometer method and compared to mock treated cells using a One-way ANOVA.

Virus Binding Study

To assess the influence of AgNPs in the binding of DENV to target cells, a cold-binding study was conducted. The first steps in the viral life cycle are binding to a target cells and entry into that cell by virus-dependent mechanisms. DENV is able to undergo cell-binding events at 4^{o}C but entry (by clatherin-mediated endocytosis) is not permitted at this low temperature.

Vero cells were seeded at $3x10^4$ cells/well in a 12-well μ-slide (Ibidi$^{(R)}$) for 24 hours. Experimental treatments (AgNP-DENV, DENV, and AgNP) were prepared at room temperature for one hour. The AgNP-treated DENV treatment was co-incubated for one hour at room temperature to permit binding of AgNP to DENV. Volumes of AgNP and DENV used in the co-incubation were calculated to provide the desired AgNP concentration and DENV multiplicity of infection (MOI). The required virus inoculum was calculated using the formula:

$$\frac{(cells\ per\ well)(MOI)}{(virus\ titer, pfu)} * 1000\mu L = (innoculum)\mu L$$

Cells and treatments were cooled to 4ºC for 15 minutes. The treatments were incubated with cells for one hour at 4ºC. Slides were gently rocked every 15 minutes during treatment. Following cold incubation, cells were gently washed three times with PBS (4ºC) to remove unbound DENV and/or AgNP. Control cells were also washed in the same manner. Treatments and washes were removed by pouring onto an absorbent towel.[1] Cells were fixed with chilled 4% paraformaldehyde to prevent the internalization of DENV and AgNP. Indirect fluorescence (without Triton-X permeabilization) was performed to visualize the effects of AgNP on DENV binding to target cells.

Cells were washed three times with PBS. Primary antibody was diluted 1:300 per manufacturer specifications and incubated with cells for one hour at 37ºC or overnight at 4ºC. The primary antibody used was the Anti-Dengue Virus Serotype 2 Antibody, clone 3H5-1 of mouse origin (MAB8702 Chemicon, Hampshire, United Kingdom). As an isotype control, normal mouse IgG (NI03, Calbiochem®) was added in place of the 3H5 in one well.

Following incubation, the primary antibody was removed and cells were washed three times with chilled PBS. Secondary antibody was diluted and added to cells for one hour at 37ºC or overnight at 4ºC. The secondary antibody was rabbit anti-mouse IgG-FITC. The secondary antibody was removed and cells washed three times with chilled PBS. Cells were counter-stained with Texas Red®-X Phalloidin for 10 minutes to

[1] Vacuum aspiration repeatedly removed cells in early trials

visualize the polymerized F-actin cytoskeleton of the cells. Cells were washed three times with chilled PBS and a cover slip was mounted using Vectashield® H-1500 which contains DAPI (4',6-diamidino-2-phenylindole, blue) for nuclear visualization.

Visualization was performed on an Olympus inverted fluorescence microscope with a CytoViva® Dual Mode Fluorescence system, which provided enhanced visualization of the AgNP. Exposure time required for image capture varied for each fluorescent stain. The optimal values found for these assays were TRITC (tetramethylrhodamine, red) 500ms and FITC (Fluorescein isothiocyanate, green) 1900ms. Optical and software settings were identical when capturing images and not enhanced to artificially increase or decrease fluorescence.

Blocking Non-Specific Binding During Immunofluorescence

During indirect immunofluorescence procedures, the decision was made to exclude the common blocking step. Traditionally, cells are incubated with bovine serum albumin (BSA) and serum matching the host of the secondary antibody to block the non-specific binding of antibodies to cell Fc receptors. According to research by Igor Buchwalow, et al, there were no significant differences between various samples that received or did not receive blocking treatment [23]. Buchwalow demonstrated that the standard fixation step removes the ability of endogenous Fc receptors to bind the Fc portion of antibodies. This result was confirmed during early fluorescence trials where blocked and non-blocked samples were compared under the same experimental conditions. In the absence of blocking, background staining was never observed. This

decision saved time and lab resources and add further credibility to the suggestion that protein blocking steps, although commonplace in laboratories, are unnecessary.

Image Processing and Analysis

For purposes of this research and the virus binding study, the green (FITC) fluorescent intensity represents the level of DENV attachment to the surface of Vero cells. Image processing methods were used to isolate the fluorescent region of interest (ROI) and remove the background and artifacts. Image analysis methods were used to quantify the differences between ROI. The relative difference in fluorescence intensity between images provided quantifiable differences between the level of DENV binding to cells. Immunofluorescent images were processed and analyzed in Image J (National Institutes of Health, http://Image J.nih.gov/ij/). Detailed screenshots of the image processing and analysis steps are contained in Appendix B. Image processing and analysis was conducted using procedures established for the quantification of fluorescence, which are accepted within the microscopy community.

The aim of the image processing steps is to isolate the fluorescence that best represents the presence of DENV bound to cell surface receptors. Processing is based on the concept of lookup tables (LUT). Within Image J, a color image is converted to an 8-bit image. A single color (green) 8-bit LUT represents 256 possible shades (bins) of green. A LUT value of zero represent black and 255 represents pure green. The fluorescent ROI falls between bins 0-255 but would be impossible to identify with the naked eye. The image processing and analysis steps are described below and summarized in Figure 8:

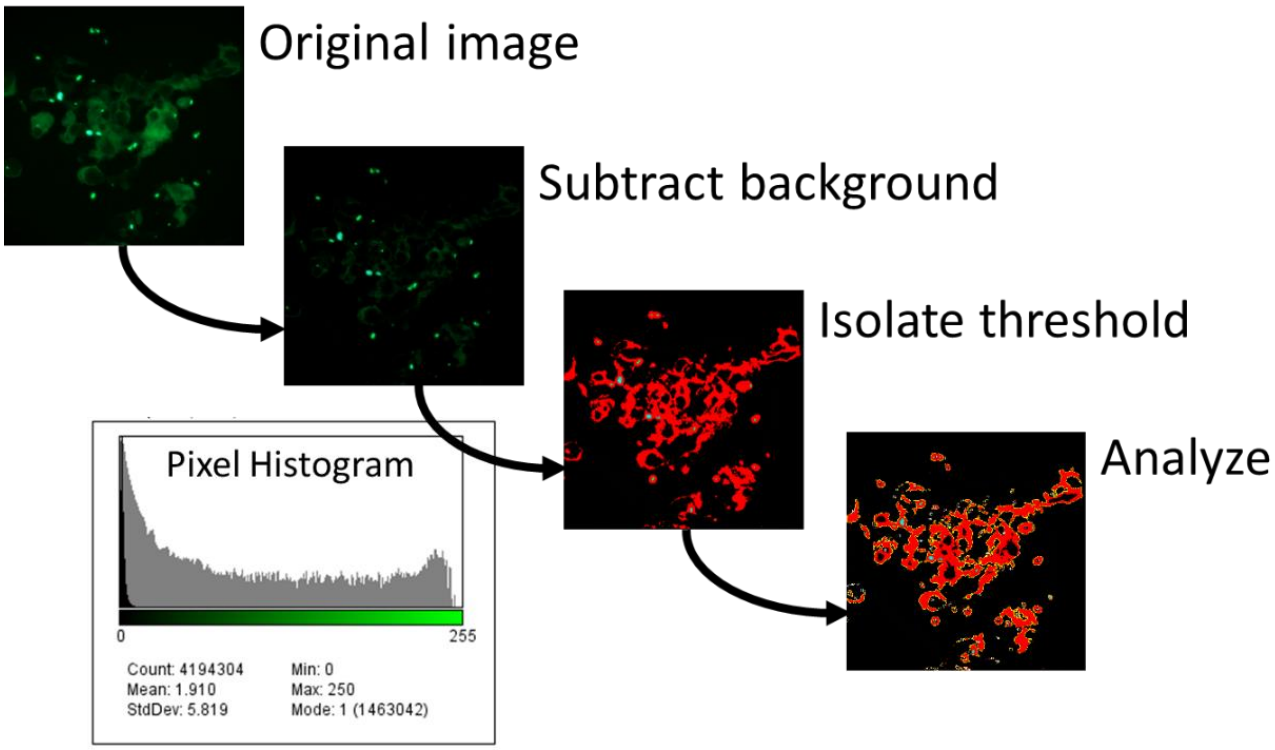

Figure 8. Image processing and analysis overview

1. Convert single-color image to 8-bit. While other image depths are available (i.e. 24-bit, with range 0-4095), the additional resolution is not required for this analysis.

2. Subtract background. Background subtraction is extremely important when quantifying image intensities. This operation removes constant pixel information from a continuous background (Figure 9). This does not remove the presence of fluorescent artifacts (Figure 10). Artifacts represent areas with high intensity that were not caused by the binding of fluorescently-tagged secondary antibodies to DENV (actually to the primary antibodies bound to DENV E-protein). If artifacts are included in the analysis,

they would skew the results and represent greater levels of bound DENV than there truly are.

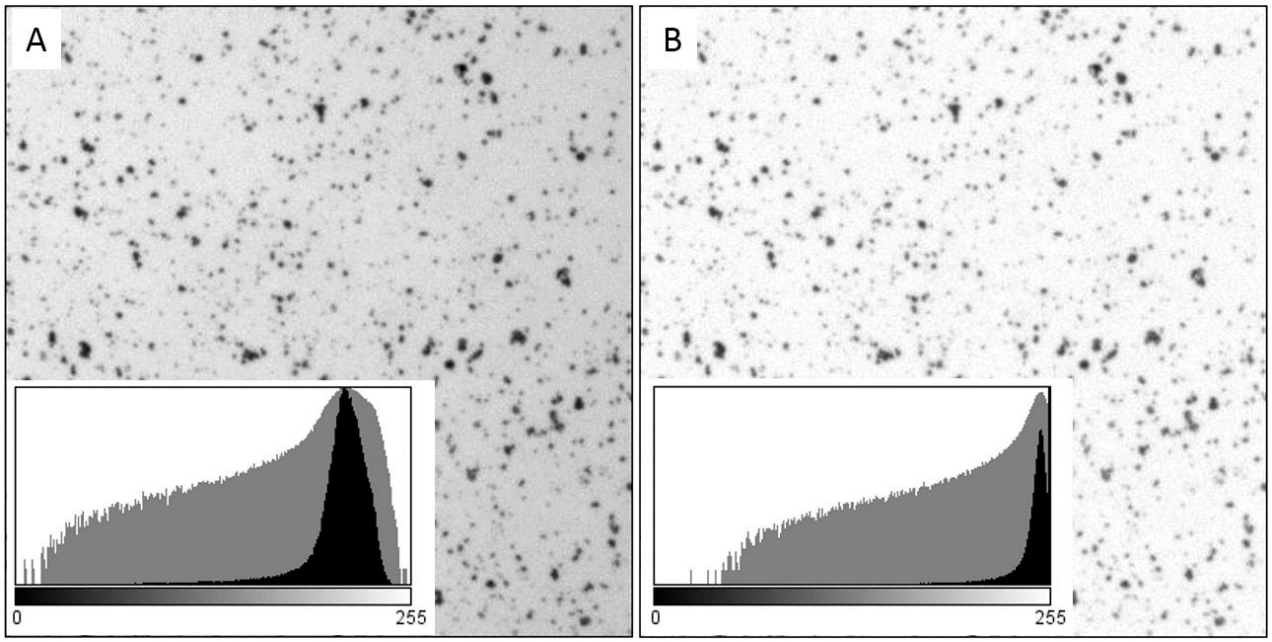

Figure 9. Sample background subtraction in Image J. A) Original greyscale image and histogram, B) Image with background subtracted and associated changes to the histogram.

3. Identify exclusion regions. Before measuring the fluorescence intensity of an image, the pixel values (bins 0-255) of the exclusion regions must be identified. The two exclusion regions are the black background and the bight, saturated artifacts. The pixel values representative of these regions are identified through the histograms of selection areas that only include the area types to exclude. Image histograms graphically represent the number of occurrences of each pixel value, with each pixel providing one count. Analyzing the pixel values of black areas far from an ROI will provide the pixel values representing black background. Analyzing the pixel values of highly saturated artifacts will provide the pixel values representing false fluorescence intensity that needs to be excluded from final analysis (Figure 10). Repeated measurements identified that pixel

values from 0-8 represent black and values from 198-255 are present only in the artifacts. In each image, the final range of pixel values representing the ROI were bins 9-197.

4. Isolate the threshold (ROI) using the limits of black maximum and artifact minimum. Within the Image J Threshold feature, the pixel values are set to the 9-197 range mentioned above. Thresholding the image to this range creates a binary image where excluded pixels are given a value of 0 and included pixels are given a value of 255. At this point, the image is composed of area that will or will not be included in analysis. This technique does not differentiate between strong fluorescence and weak fluorescence

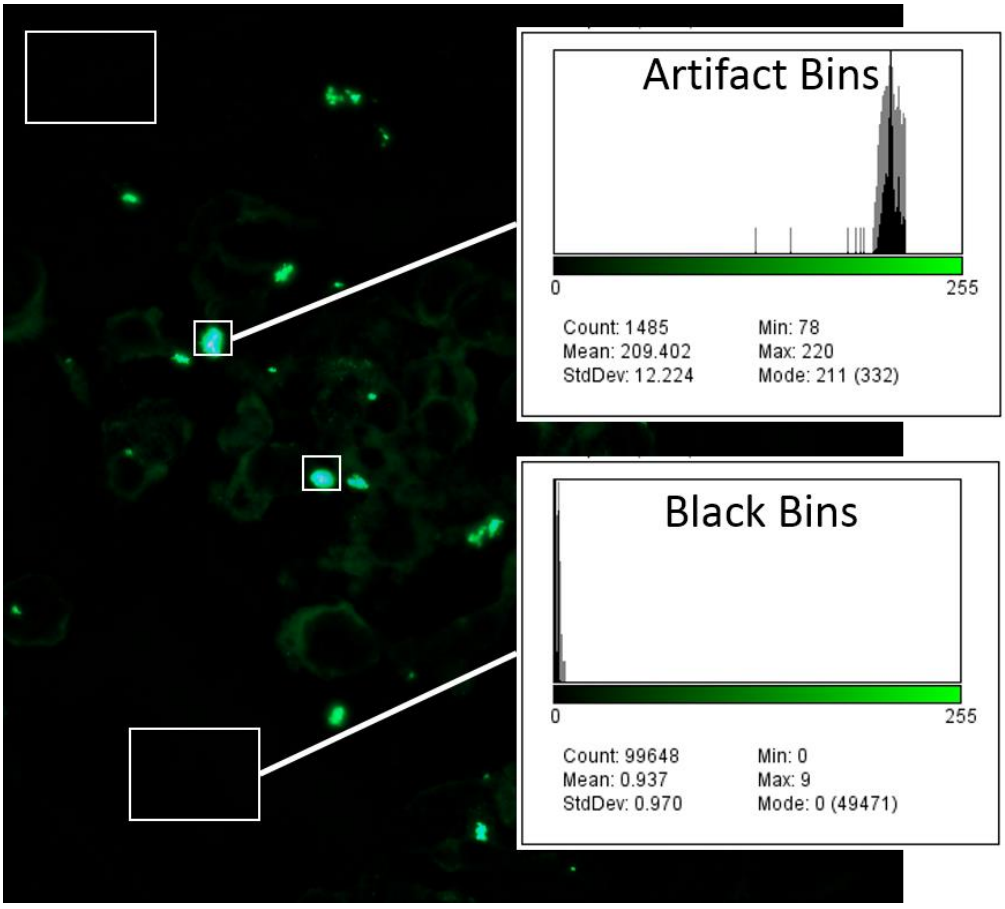

Figure 10. Identification of exclusion regions for black and artifact intensity.

directly, but is used to determine the visible surface area that contains fluorescent values (from original image) determined to be valid intensities. The qualifying area represents the ROI. The thresholding function creates closed objects within which is a portion of the total ROI. Image analysis techniques are next used to measure the total area contained within these ROI "islands" and other properties related to size and distribution.

5. Analyze images. The target metrics are total ROI area (sq. pixels) and cell count. The Measure Particles function within Image J calculates the area of individual ROI islands and provides an image total. Knowing the total area in the image that contained qualifying pixel intensity is required, but does not present the whole story. If the pixel intensity is held constant, an image with more cells should have greater area of ROI. Normalizing an image's ROI area with cell count provides a more accurate estimate of DENV binding per cell. The Cell Counter tool was utilized to count the number of cells in each image. If the normalized region of interest (nROI) is reduced from one image to the next, it is reasonable to conclude that only the different experimental conditions contributed to the reduction.

RESULTS & DISCUSSION

Characterization of AgNP

AgNP were synthesized with the Creighton method and filtered with 10kD TFF (Figure 11). Prior to filtration, the colloid was represented by a wide distribution of sizes from 1-60 nm primarily in the 6-25 nm range. After 10kD TFF, the distribution was narrowed and consisted of over 40% in the 6-10 nm range. These AgNPs presented a zeta potential of -30mV (Figure 12) and did not agglomerate before use. The colloid was estimated to have very low concentrations of silver ions (Ag+) after TFF based on

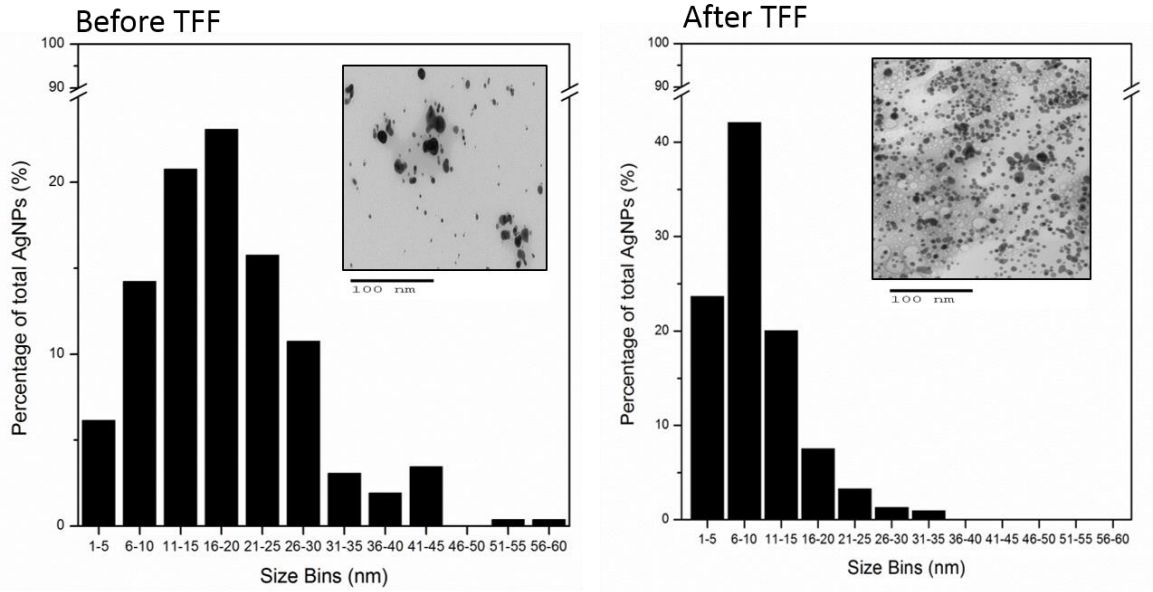

Figure 11. AgNP size distributions before and after tangential flow filtration (TFF, 10kD retentate). Visualized under TEM 80kx and measured with Image J.

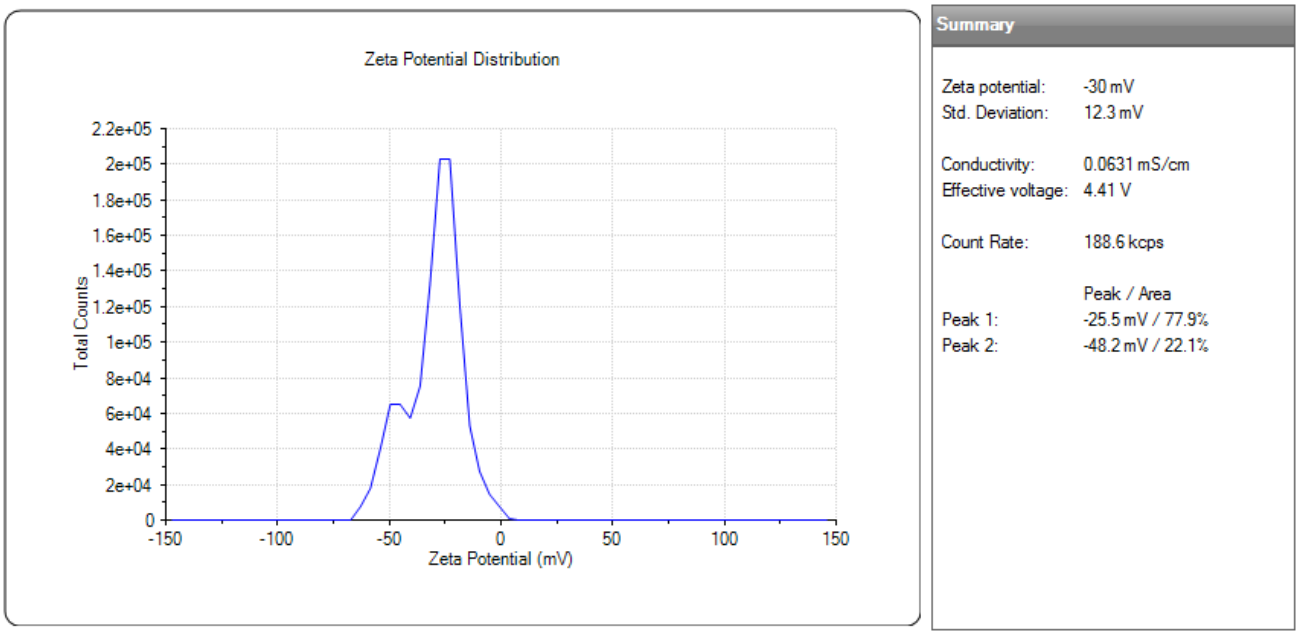

Figure 12. Creighton AgNP zeta potential

external calibration compared to the reference standard silver nitrate (AgNO3) through ICP-OES (Supplemental Figure 3). TFF was an effective and efficient technique for preparing AgNPs for this study of viral inhibition. The narrowing of AgNPs' size distribution and the removal of silver ions were critical benefits of TFF.

The AgNPs utilized for this research exhibited the characteristic UV-Vis peak at 400 nm (Figure 13). This peak was measured periodically throughout the research to confirm colloid stability.

Cytotoxicity of DENV infection in Vero cells

The effect of DENV infection of Vero cells was analyzed to confirm the infectivity of DENV virus stock and serve as a baseline for virus inhibition studies. Following 36 hours of growth, DENV-infected cells (MOI 0.1) presented 88% viability compared to non-infected cells (Figure 14). Relative Vero cell viability decreased

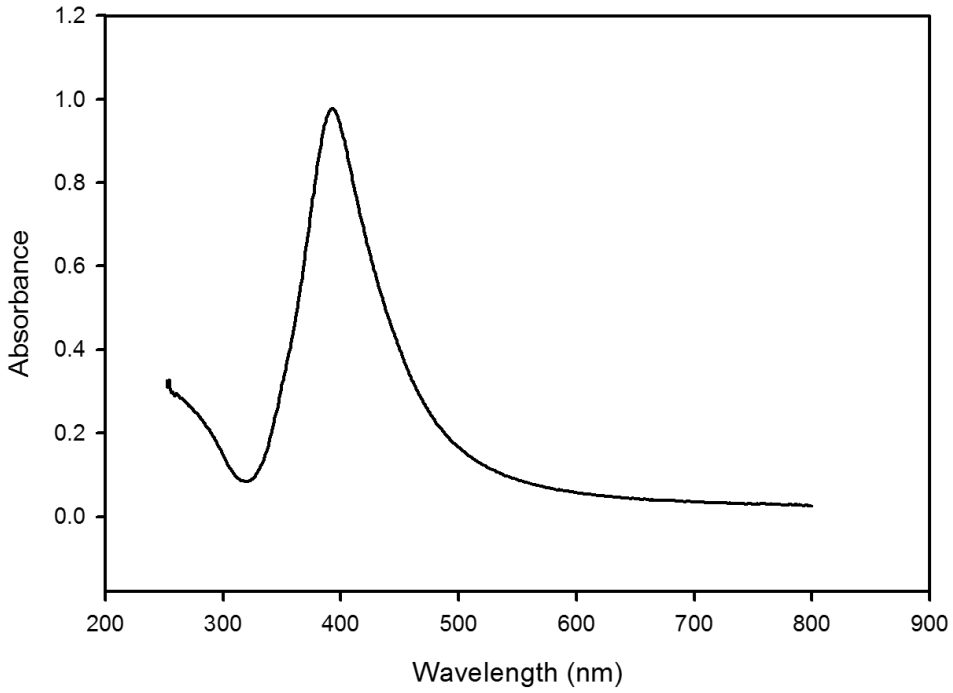

Figure 13. UV-Vis spectra for the AgNP colloid utilized in binding inhibition assay.

rapidly from 36-72 hours when infected cells were 29% viable compared to non-infected cells. By 120 hours of growth, the viability of infected and noninfected cells were comparatively low. Based on visual comparison, the infected cells experienced DENV-induced cytopathic effects and had lifted from the growth surface in patches. The noninfected cells had naturally overgrown, become weakly adherent to the growth surface, and were removed from the wells by the gentle force of media aspiration.

This decline in cell viability was expected, as Vero cells do not have innate defenses against infection. Since Vero cells are highly permissible of DENV infection, they are commonly used to propagate DENV stock during research.

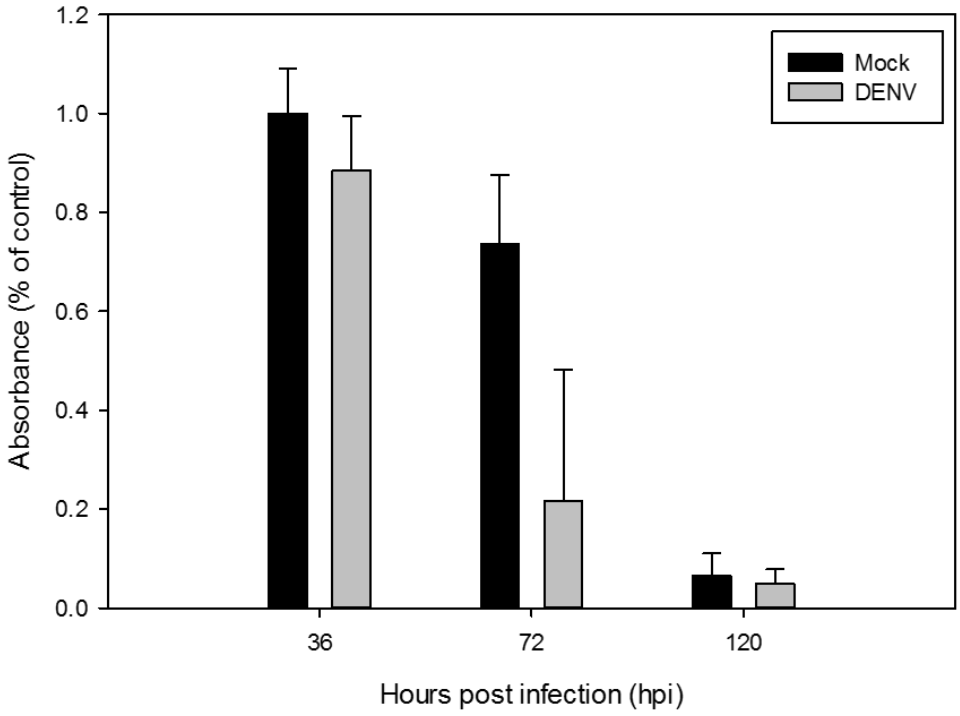

Figure 14. Viability of DENV infected Vero cells.

Biocompatibility of AgNPs in Vero cells

Cell viability measured by MTT assay demonstrated that increasing the concentration of AgNP from 10-100 µg/mL decreases cell viability relative to mock treated cells (Figure 15). Positive controls (silver ions, Ag^{+}) in the same concentrations yielded much greater cytotoxicity than AgNP, with the exception of Ag^{+} (10 µg/mL), which had higher viability than AgNP. The results suggest that AgNP stock colloid does not have a high concentration of silver ions and that AgNP concentrations should be selected to be as low as possible to minimize cytotoxic effects while providing antiviral or cytoprotective effect. Cell viability of 10 µg/mL treatments were lower than expected. In retrospect, this is likely due to the greater volume of water used to dilute the AgNP. Greater amounts of water likely altered the osmotic conditions of the cells. Further

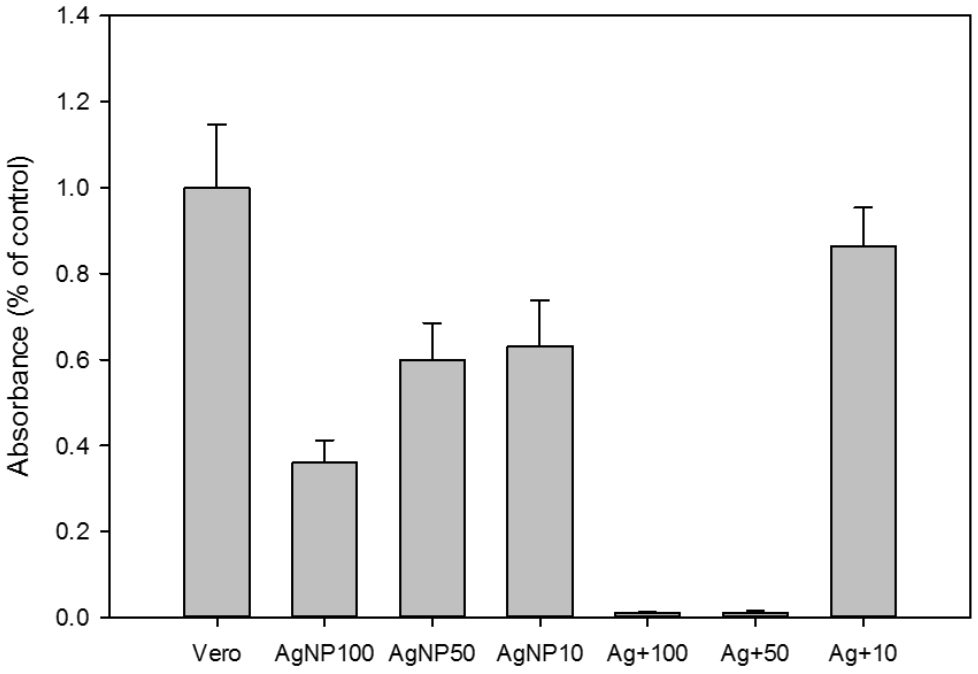

Figure 15. Cytotoxicity of silver nanoparticles (AgNP) versus silver ions (Ag+) at in concentrations of 100 µg/mL, 50 µg/mL, and 10 µg/mL.

studies used DMEM-10 for dilutions instead of water. UV-VIS analysis indicated AgNP were rapidly stabilized in DMEM-10 for the typical 1 hour treatment.

Transmission Electron Microscopy

TEM analysis of 10 µg/mL AgNPs and 25 µg/mL AgNPs incubated with DENV ($5.5x10^5$ pfu/mL) indicated that AgNPs tend to associate with virus particles (Figure 16). Under these conditions, AgNPs did not appear to bind consistently to DENV or in a particular pattern when on the viral envelope. Due to the restrictions of TEM image analysis, it is not possible to determine if the AgNP are bound to DENV or are merely in the same back focal plane. This result is inconsistent with the potential for AgNP acting as a direct antiviral by binding to the viral envelope and inhibiting virus binding and entry. It is possible that the TEM sample preparation caused some of the AgNP to shift

away from the DENV. Future experiments should utilize ethanol preparation and resin embedding for enhanced visualization.

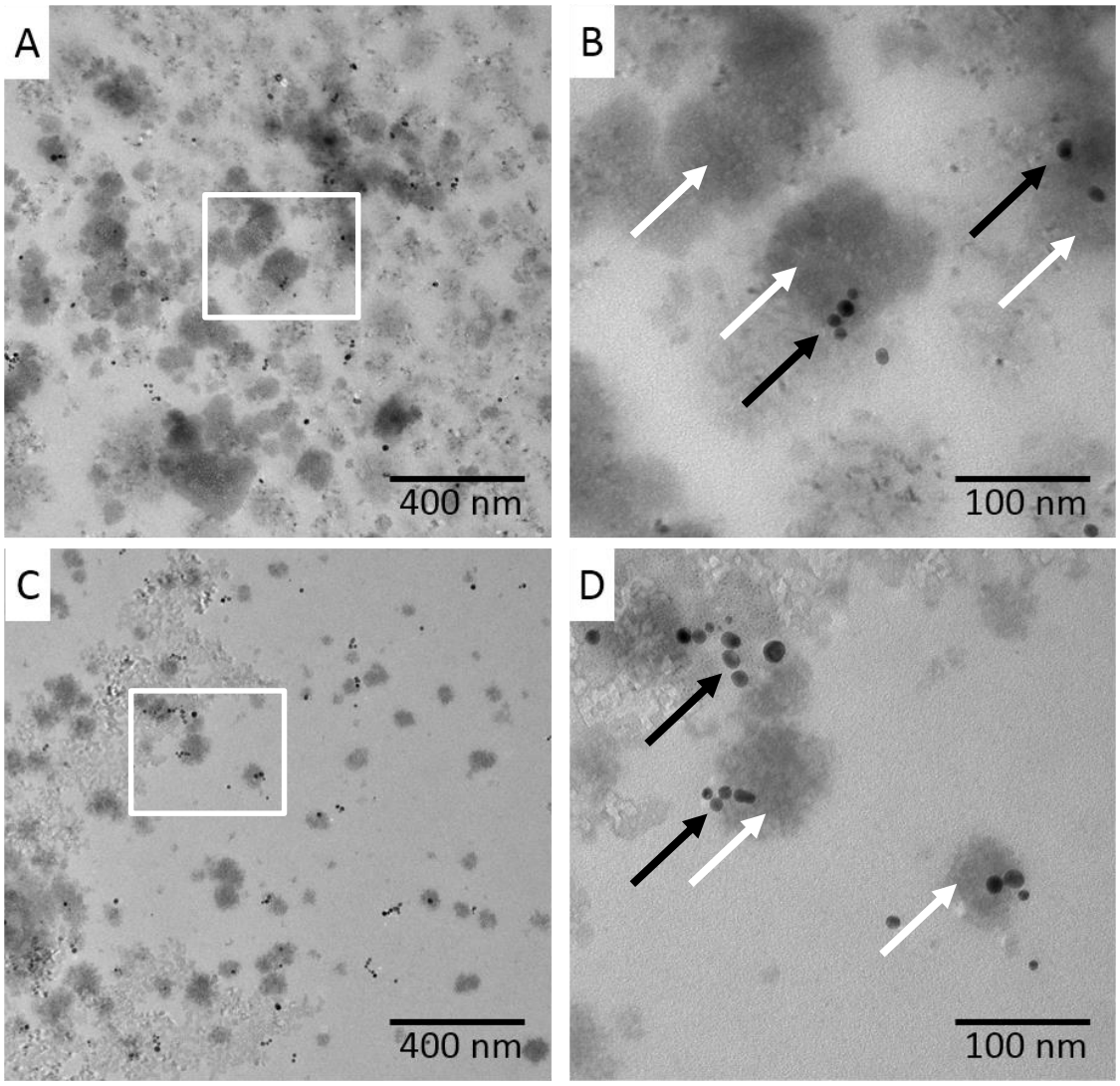

Figure 16. TEM micrographs of AgNP-DENV after 1 h incubation. 10 µg/mL AgNP A) 30kx B) 120kx, 25 µg/mL AgNP C) 30kx D) 120kx. White arrows indicate DENV virion and black arrows indicate AgNP.

Infection with DENV progeny following exposure to AgNP

AgNP treatment neutralized DENV infection of Vero cells (Figure 17). Vero cells which were infected with progeny virus from DENV that was treated with AgNP (10 µg/mL or 25 µg/mL) had viability equivalent to the mock-treated control (P>0.05). Infection with DENV progeny from first-round untreated DENV resulted in statistically significant reduction in cell viability after 3 days of growth compared to the mock control and both AgNP treatments (P<0.001, R-sq=70.4%). These results indicate that the first-round treatment of DENV with AgNP resulted in conditions which permitted higher cell viability during the second-round of treatments. On average, the Vero cells that were infected with AgNP-treated DENV were 7±0.25% more viable than the untreated DENV.

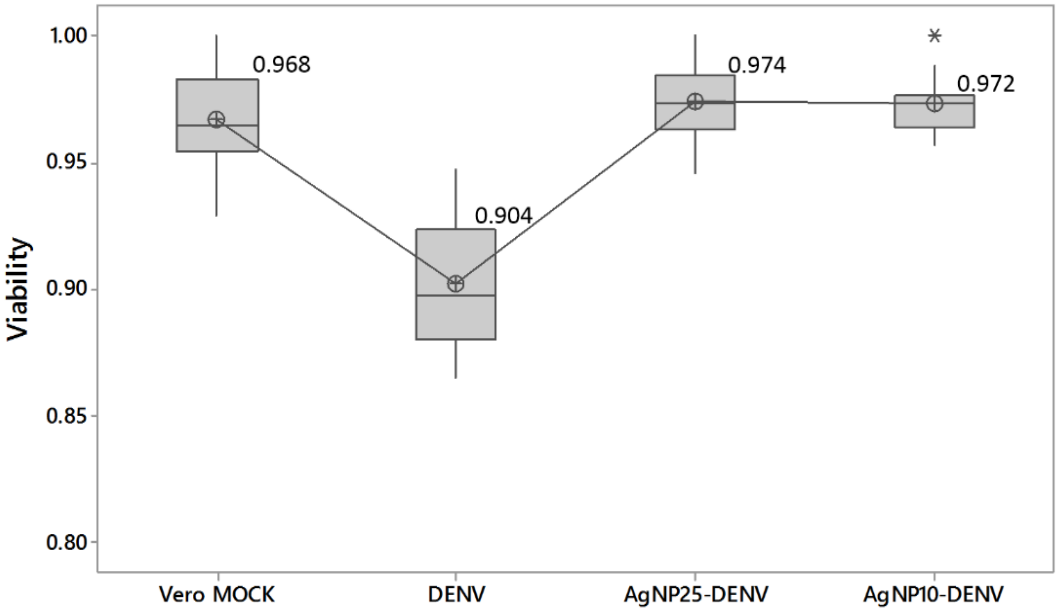

Figure 17. Boxplot of Vero cell viability after DENV progeny infection. AgNP treatment of DENV was equivalent to mock-treated control (P<0.001). Untreated DENV resulted in significantly lower cell viability than control and AgNP treatments (P>0.05). Result from One-way ANOVA. (* denotes an outlier in the data)

This may be due to decreased mature DENV production in Vero cells during the first-round.

AgNP Influence on RAW Cell Viability during DENV Infection

DENV binding to RAW cells was isolated and measured. DENV is able to undergo cell-binding events at 4ºC but entry (by clatherin-mediated endocytosis) is not permitted at this low temperature. RAW cells infected with AgNP-treated DENV had significantly higher cell viability 3 days post infection ($P<0.001$). On average, the RAW cells that were infected with AgNP-treated DENV (10 µg/mL or 25 µg/mL) were 7±0.59% more viable than untreated DENV (Figure 18). While this does not identify the

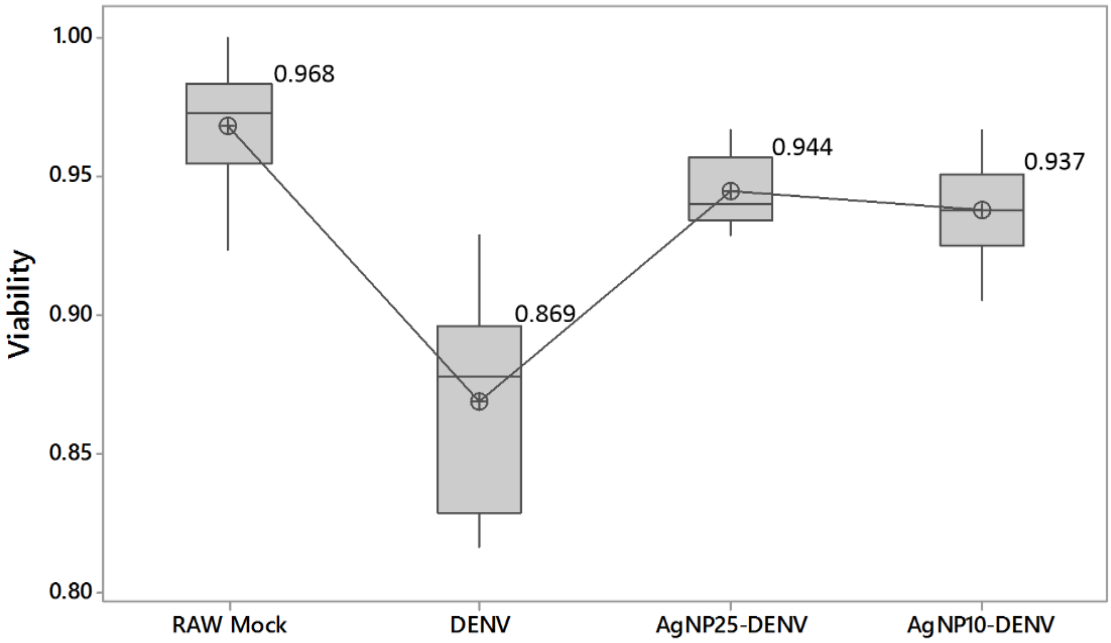

Figure 18. Boxplot of RAW cell viability after DENV infection. RAW cell viability 3 days post infection with AgNP-treated DENV (25 µg/mL) was not significantly less than mock-treated control ($P>0.05$) but was lower in the 10 µg/mL AgNP condition ($P<0.05$). Untreated DENV resulted in significantly lower cell viability than control and AgNP treatments ($P<0.05$). Result from One-way ANOVA.

mechanism of viral inhibition, it provides evidence that AgNPs support cell viability during viral challenge.

AgNP Inhibition of DENV Binding to RAW Cells

An indirect immunofluorescence protocol similar to *AgNP Inhibition of DENV Binding to Vero Cells* was performed using citrate stabilized AgNPs and RAW cells. Fluorescent image analysis revealed that 8 µg/mL AgNP pretreatment of DENV reduced the fluorescence intensity (per cell) by 38±5.3% (Figure 19, Figure 20). It is possible that

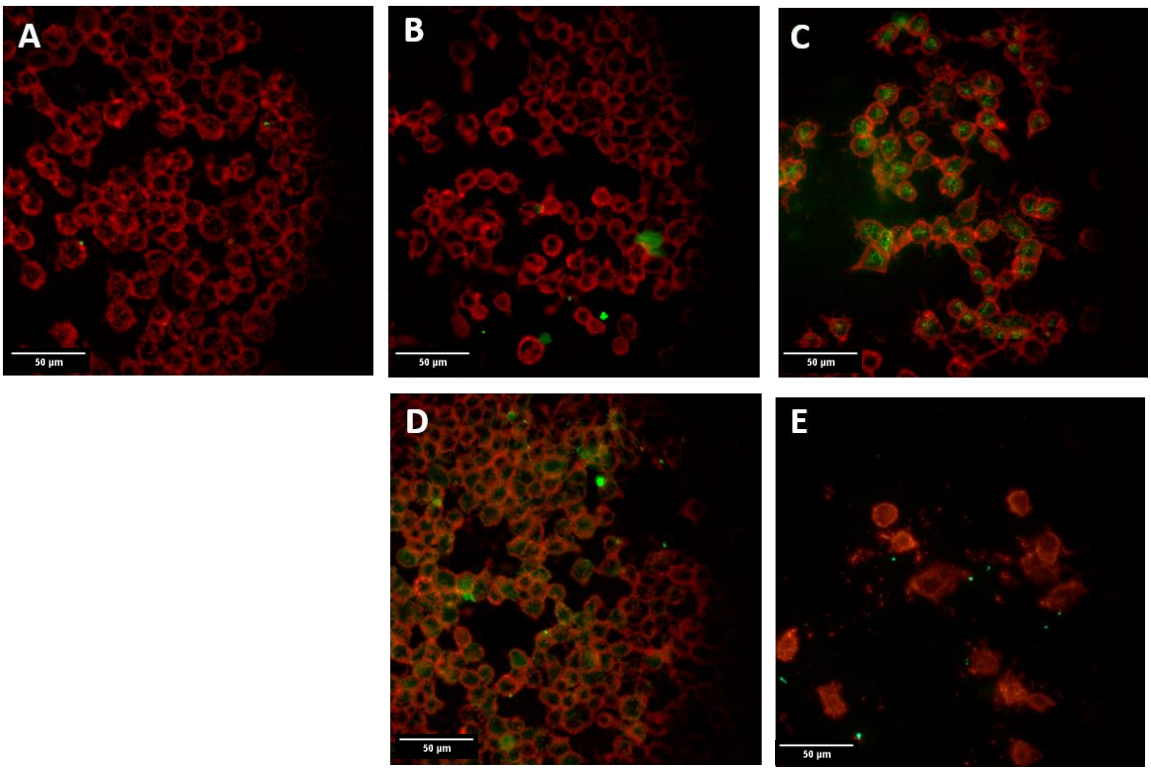

Figure 19. AgNP treatment blocks binding of DENV to RAW cells. A) mock treated, no AgNP or DENV B) isotype control, normal mouse IgG, no AgNP or DENV, C) DENV DENV infection of RAW cells without AgNP treatment (MOI 10), D) DENV binding inhibited by pre-treatment with AgNP (8 µg/mL), E) AgNP treatment with RAW cells and no DENV (8 µg/mL). Green fluorescence (FITC, DENV E protein) and red fluorescence (TRITC, f-actin). Images enhanced +40% brightness, -40% contrast for better viewing in print. Scale bar: 50µm.

DENV may be in the same area as receptors, but not bound to it. It is difficult to say that DENV is absolutely bound to the receptor by using microscopy. Additional studies could

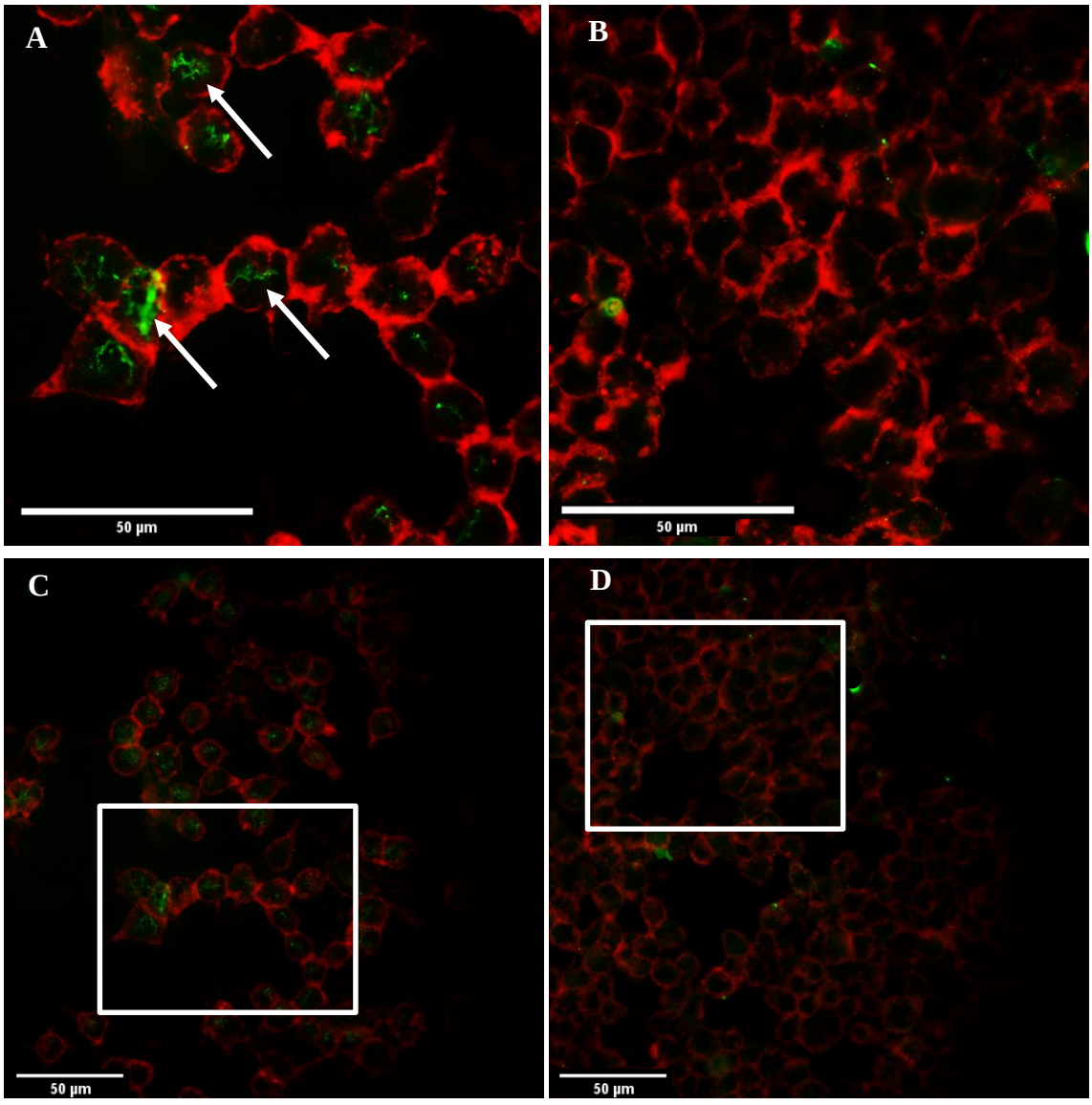

Figure 20. AgNP treatment blocks binding of DENV to RAW cells. (A) DENV binding to RAW cells without AgNP treatment (magnified), white arrows indicate DENV bound to RAW surface receptors, (B) DENV binding inhibited by pre-treatment with AgNP (8 µg/mL). Green fluorescence (FITC, DENV E protein) and red fluorescence (TRITC, f-actin). Image brightness and contrast enhanced 40% for better viewing in print (A & B). (C & D) Non-enhanced composites, 60x magnification. Scale bar: 50µm.

use co-immunoprecipitation with SDS-PAGE and Western blot analysis to identify the binding properties of the AgNP-DENV-receptor complex.

Statistical Analysis

SigmaPlot 12.5 (Systat & Mystat Products, Chicago, IL) and Minitab 17 (Minitab Inc., State College, PA) were used to create graphs and perform statistical analysis. One-way ANOVA was used to evaluate differences between experimental results when normality and equal variance criteria were met. Experimental conditions were compared to mock-treated controls as percent of control. Isotype controls to remove the influence of background fluorescence from cellular autofluorescence and non-antigen-specific binding. Image J was used to process images for statistical analysis as described above.

Histograms representing fluorescence intensities within the ROI were compared using the Mann-Whitney rank sum test. As expected, each histogram failed the normality test (Shapiro-Wilk), therefore, the Mann-Whitney rank sum test provided greater descriptive efficiency than the paired t test.

CONCLUSION

The null hypothesis of this study was that silver nanoparticles do not inhibit the replication cycle of dengue virus serotype 2 (DENV2) in Vero 76 and RAW cells. Results indicate that AgNP-pretreated DENV produced a statistically significant reduction in fluorescence intensity compared to DENV infection without AgNP pretreatment ($P<0.05$). Results also indicate that AgNP-pretreated DENV produced statistically significant increases in cell viability (average 7%) in Vero and RAW cells

compared to DENV infection without AgNP pretreatment ($P<0.05$). Therefore, the null hypothesis is rejected.

This research presents, for the first time that DENV binding and replication in Vero and RAW cells is inhibited by 6-10 nm AgNPs (Creighton). A limitation of this study is that the mechanism of binding inhibition is unknown. Existing knowledge on AgNP interaction with viral envelopes suggests that AgNPs bind to DENV disulfide regions and possibly others. This could inhibit binding by preventing receptor-epitope binding. It is also possible that AgNPs prevent the formation of a membrane fusion complex between internalized DENV and the late endosome, leading to reduced viral progeny and sustained cell viability. It has been suggested that unbound AgNPs in the AgNP-DENV colloid coat the cells and prevent DENV binding in a cytoprotective manner, rather than as an antiviral agent. This could be examined by incubating cells with AgNPs prior to DENV infection, although one study found no altered viral inhibition with this method [41].

This serves as a stepping off point for further research into the interaction of AgNPs and DENV. Continued research could include:

- Development of a technique to filter unbound AgNPs from the AgNP-DENV colloid to prevent unbound AgNPs from binding to cells
- Co-immunoprecipitation to identify the binding properties of AgNP-DENV-receptor complexes

- Measure cell viability throughout the course of DENV infection versus AgNP-DENV, measured by MTT assay
- Uses of AgNPs to disrupt the disease cycle in *Aedes* mosquitoes
- Progeny virus production following AgNP-treated DENV infection of Vero cells or macrophages, measured by using supernatants from infected cultures to infect second set of cell cultures, quantified by either flow cytometry or MTT assay
- Changes in DENV protein production, measured through Western blot after DENV infection
- Impact of AgNPs during DENV infection of macrophages (target cells)
- Quantification of DENV infection after AgNPs treatment, measured by flow cytometry

REFERENCES

[1] A. P. Goncalvez, R. E. Engle, M. St Claire, R. H. Purcell, and C.-J. Lai, "Monoclonal antibody-mediated enhancement of dengue virus infection in vitro and in vivo and strategies for prevention.," *Proc. Natl. Acad. Sci. U. S. A.*, vol. 104, no. 22, pp. 9422–7, May 2007.

[2] WHO, "Dengue and severe dengue," 2014. [Online]. Available: http://www.who.int/mediacentre/factsheets/fs117/en/.

[3] CDC, "Dengue Epidemiology," 2014. [Online]. Available: http://www.cdc.gov/dengue/epidemiology/index.html. [Accessed: 09-Jan-2015].

[4] E. A. Henchal and J. R. Putnak, "The Dengue Viruses," vol. 3, no. 4, pp. 376–396, 1990.

[5] D. J. Gubler, "Epidemic dengue/dengue hemorrhagic fever as a public health, social and economic problem in the 21st century.," *Trends Microbiol.*, vol. 10, no. 2, pp. 100–3, Mar. 2002.

[6] M. M. Wade, A. E. Chambers, J. M. Insalaco, and A. W. Zulich, "Survival of viral biowarfare agents in disinfected waters.," *Int. J. Microbiol.*, vol. 2010, p. 412694, Jan. 2010.

[7] M. S. Mustafa, V. Rasotgi, S. Jain, and V. Gupta, "Discovery of fifth serotype of dengue virus (DENV-5): A new public health dilemma in dengue control," *Med. J. Armed Forces India*, vol. 71, no. 1, pp. 67–70, 2015.

[8] E. a Henchal and J. R. Putnak, "The dengue viruses.," *Clin. Microbiol. Rev.*, vol. 3, no. 4, pp. 376–96, Oct. 1990.

[9] World Health Organization, "Dengue: guidelines for diagnosis, treatment, prevention, and control," *Spec. Program. Res. Train. Trop. Dis.*, pp. x, 147, 2009.

[10] J. Hombach, M. Jane Cardosa, A. Sabchareon, D. W. Vaughn, and A. D. T. Barrett, "Scientific consultation on immunological correlates of protection induced by dengue vaccines. Report from a meeting held at the World Health Organization 17-18 November 2005," in *Vaccine*, 2007, vol. 25, pp. 4130–4139.

[11] S. Shresta, K. L. Sharar, D. M. Prigozhin, P. R. Beatty, and E. Harris, "Murine model for dengue virus-induced lethal disease with increased vascular permeability.," *J. Virol.*, vol. 80, no. 20, pp. 10208–10217, 2006.

[12] L. Yauch and S. Shresta, “Mouse models of dengue virus infection and disease,” *NIH Public Access*, vol. 80, no. 2, pp. 87–93, 2011.

[13] B. L. Innis, K. H. Eckels, E. Kraiselburd, D. R. Dubois, G. F. Meadors, D. J. Gubler, D. S. Burke, and W. H. Bancroft, “Virulence of a live dengue virus vaccine candidate: a possible new marker of dengue virus attenuation.,” *J. Infect. Dis.*, vol. 158, pp. 876–880, 1988.

[14] T. L. Yap, T. Xu, Y.-L. Chen, H. Malet, M.-P. Egloff, B. Canard, S. G. Vasudevan, and J. Lescar, “Crystal structure of the dengue virus RNA-dependent RNA polymerase catalytic domain at 1.85-angstrom resolution.,” *J. Virol.*, vol. 81, no. 9, pp. 4753–65, May 2007.

[15] Z. Yin, Y. Chen, W. Schul, Q. Wang, F. Gu, J. Duraiswamy, W. Liu, B. Liu, J. Y. H. Lim, C. Young, M. Qing, C. Chin, A. Yip, G. Wang, W. Ling, H. Pen, K. Lin, B. Zhang, G. Zou, K. A. Bernard, C. Garrett, K. Beltz, M. Dong, M. Weaver, H. He, A. Pichota, V. Dartois, T. H. Keller, and P. Shi, “An adenosine nucleoside inhibitor of dengue virus,” 2009.

[16] A. C. Eifler and C. S. Thaxton, “Nanoparticle therapeutics: FDA approval, clinical trials, regulatory pathways, and case study.,” *Methods Mol. Biol.*, vol. 726, pp. 325–38, Jan. 2011.

[17] A. M. Schrand, M. F. Rahman, S. M. Hussain, J. J. Schlager, D. a Smith, and A. F. Syed, “Metal-based nanoparticles and their toxicity assessment.,” *Wiley Interdiscip. Rev. Nanomed. Nanobiotechnol.*, vol. 2, no. 5, pp. 544–68, 2010.

[18] R. J. Vandebriel, E. C. Tonk, L. J. de la Fonteyne-Blankestijn, E. R. Gremmer, H. W. Verharen, L. T. van der Ven, H. van Loveren, and W. H. de Jong, “Immunotoxicity of silver nanoparticles in an intravenous 28-day repeated-dose toxicity study in rats.,” *Part. Fibre Toxicol.*, vol. 11, no. 1, p. 21, Jan. 2014.

[19] J. S. Kim, J. H. Sung, J. H. Ji, K. S. Song, J. H. Lee, C. S. Kang, and I. J. Yu, “In vivo Genotoxicity of Silver Nanoparticles after 90-day Silver Nanoparticle Inhalation Exposure.,” *Saf. Health Work*, vol. 2, no. 1, pp. 34–8, Mar. 2011.

[20] J. H. Lee, Y. S. Kim, K. S. Song, H. R. Ryu, J. H. Sung, J. D. Park, H. M. Park, N. W. Song, B. S. Shin, D. Marshak, K. Ahn, J. E. Lee, and I. J. Yu, “Biopersistence of silver nanoparticles in tissues from Sprague-Dawley rats.,” *Part. Fibre Toxicol.*, vol. 10, p. 36, Jan. 2013.

[21] I. Papageorgiou, C. Brown, R. Schins, S. Singh, R. Newson, S. Davis, J. Fisher, E. Ingham, and C. P. Case, “The effect of nano- and micron-sized particles of cobalt-

chromium alloy on human fibroblasts in vitro.," *Biomaterials*, vol. 28, no. 19, pp. 2946–58, Jul. 2007.

[22] L. Schnirring, "Researchers identify fifth dengue serotype," *CIDRAP News*, 2013. [Online]. Available: http://www.cidrap.umn.edu/news-perspective/2013/10/researchers-identify-fifth-dengue-subtype.

[23] C. Moore, "UTMB Galveston Researchers Discover First New Dengue Fever Serotype In 50 Years," *BioNews Texas*, 2013. [Online]. Available: http://bionews-tx.com/news/2013/10/25/utmb-galveston-researchers-discover-first-new-dengue-fever-serotype-in-50-years/.

[24] M. G. Guzmán and G. Kourí, "Dengue: an update.," *Lancet. Infect. Dis.*, vol. 2, no. 1, pp. 33–42, Jan. 2002.

[25] J. Blok, "Genetic Relationships of the Dengue Virus Serotypes," pp. 1323–1325, 1985.

[26] R. J. Kuhn, W. Zhang, M. G. Rossmann, S. V Pletnev, J. Corver, E. Lenches, C. T. Jones, S. Mukhopadhyay, P. R. Chipman, E. G. Strauss, T. S. Baker, and J. H. Strauss, "Structure of dengue virus: implications for flavivirus organization, maturation, and fusion.," *Cell*, vol. 108, no. 5, pp. 717–25, Mar. 2002.

[27] Y. Modis, S. Ogata, D. Clements, and S. C. Harrison, "A ligand-binding pocket in the dengue virus envelope glycoprotein.," *Proc. Natl. Acad. Sci. U. S. A.*, vol. 100, no. 12, pp. 6986–91, Jun. 2003.

[28] F. Medina, J. F. Medina, C. Colón, E. Vergne, G. A. Santiago, and J. L. Muñoz-Jordán, "Dengue virus: isolation, propagation, quantification, and storage.," *Curr. Protoc. Microbiol.*, vol. Chapter 15, no. November, p. Unit 15D.2., Nov. 2012.

[29] K. I. P. J. Hidari and T. Suzuki, "Dengue virus receptor.," *Trop. Med. Health*, vol. 39, no. 4 Suppl, pp. 37–43, Dec. 2011.

[30] K. I. P. J. Hidari and T. Suzuki, "Dengue virus receptor.," *Trop. Med. Health*, vol. 39, no. 4 Suppl, pp. 37–43, Dec. 2011.

[31] J. L. Miller, B. J. de Wet, L. Martinez-Pomares, C. M. Radcliffe, R. a Dwek, P. M. Rudd, and S. Gordon, "The mannose receptor mediates dengue virus infection of macrophages," *PLoS Pathog*, vol. 4, no. 2, p. e17, Feb. 2008.

[32] W. M. P. B. Wahala and A. M. De Silva, "The human antibody response to dengue virus infection.," *Viruses*, vol. 3, no. 12, pp. 2374–95, Dec. 2011.

[33] H. M. van der Schaar, M. J. Rust, C. Chen, H. van der Ende-Metselaar, J. Wilschut, X. Zhuang, and J. M. Smit, "Dissecting the cell entry pathway of dengue virus by single-particle tracking in living cells.," *PLoS Pathog.*, vol. 4, no. 12, p. e1000244, Dec. 2008.

[34] L. Suksanpaisan, T. Susantad, and D. R. Smith, "Characterization of dengue virus entry into HepG2 cells.," *J. Biomed. Sci.*, vol. 16, no. strain 16007, p. 17, Jan. 2009.

[35] M. N. Krishnan, B. Sukumaran, U. Pal, H. Agaisse, J. L. Murray, T. W. Hodge, and E. Fikrig, "Rab 5 is required for the cellular entry of dengue and West Nile viruses.," *J. Virol.*, vol. 81, no. 9, pp. 4881–5, May 2007.

[36] J. C. Trefry, "The development of silver nanoparticles as antiviral agents," Dayton, 2011.

[37] J. V. Rogers, C. V. Parkinson, Y. W. Choi, J. L. Speshock, and S. M. Hussain, "A Preliminary Assessment of Silver Nanoparticle Inhibition of Monkeypox Virus Plaque Formation," *Nanoscale Res. Lett.*, vol. 3, no. 4, pp. 129–133, Apr. 2008.

[38] E. A. Sopova, V. I. Baranov, O. A. Gankovskaia, V. F. Lavrov, and V. V Zverev, "Effects of silver and silicon dioxide nanopowders on the development of herpesvirus infection in vitro," *Gig. Sanit.*, pp. 89–91.

[39] D. Xiang, Q. Chen, L. Pang, and C. Zheng, "Inhibitory effects of silver nanoparticles on H1N1 influenza A virus in vitro.," *J. Virol. Methods*, vol. 178, no. 1–2, pp. 137–42, Dec. 2011.

[40] D. Xiang, Y. Zheng, W. Duan, X. Li, J. Yin, S. Shigdar, M. L. O'Connor, M. Marappan, X. Zhao, Y. Miao, B. Xiang, and C. Zheng, "Inhibition of A/Human/Hubei/3/2005 (H3N2) influenza virus infection by silver nanoparticles in vitro and in vivo," *Int. J. Nanomedicine*, vol. 8, pp. 4103–4114, 2013.

[41] J. L. Speshock, R. C. Murdock, L. K. Braydich-Stolle, A. M. Schrand, and S. M. Hussain, "Interaction of silver nanoparticles with Tacaribe virus.," *J. Nanobiotechnology*, vol. 8, p. 19, Jan. 2010.

[42] L. Sun, A. K. Singh, K. Vig, S. R. Pillai, and S. R. Singh, "Silver nanoparticles inhibit replication of respiratory syncytial virus," *J. Biomed. Nanotechnol.*, vol. 4, no. 2, pp. 149–158, 2008.

[43] H. H. Lara, N. V Ayala-Nuñez, L. Ixtepan-Turrent, and C. Rodriguez-Padilla, "Mode of antiviral action of silver nanoparticles against HIV-1.," *J. Nanobiotechnology*, vol. 8, p. 1, Jan. 2010.

[44] H. H. Lara, L. Ixtepan-Turrent, E. N. Garza Treviño, and D. K. Singh, "Use of silver nanoparticles increased inhibition of cell-associated HIV-1 infection by neutralizing antibodies developed against HIV-1 envelope proteins.," *J. Nanobiotechnology*, vol. 9, no. 1, p. 38, Jan. 2011.

[45] J. L. Elechiguerra, J. L. Burt, J. R. Morones, A. Camacho-Bragado, X. Gao, H. H. Lara, and M. J. Yacaman, "Interaction of silver nanoparticles with HIV-1.," *J. Nanobiotechnology*, vol. 3, p. 6, Jan. 2005.

[46] J. C. Trefry and D. P. Wooley, "Rapid assessment of antiviral activity and cytotoxicity of silver nanoparticles using a novel application of the tetrazolium-based colorimetric assay.," *J. Virol. Methods*, vol. 183, no. 1, pp. 19–24, Jul. 2012.

[47] L. Lu, R. W.-Y. Sun, R. Chen, C.-K. Hui, C.-M. Ho, J. M. Luk, G. K. K. Lau, and C.-M. Che, "Silver nanoparticles inhibit hepatitis B virus replication.," *Antivir. Ther.*, vol. 13, no. 2, pp. 253–62, Jan. 2008.

[48] K. Williams, "Interaction of Silver Nanoparticles with Dengue virus infection."

[49] N. Chen, Y. Zheng, J. Yin, X. Li, and C. Zheng, "Inhibitory effects of silver nanoparticles against adenovirus type 3 in vitro," *J. Virol. Methods*, vol. 193, no. 2, pp. 470–477, 2013.

[50] J. R. Furr, A. D. Russell, T. D. Turner, and A. Andrews, "Antibacterial activity of Actisorb Plus, Actisorb and silver nitrate," *J. Hosp. Infect.*, vol. 27, no. 3, pp. 201–208, Jul. 1994.

[51] J. Y. Kim, C. Lee, M. Cho, and J. Yoon, "Enhanced inactivation of E. coli and MS-2 phage by silver ions combined with UV-A and visible light irradiation," *Water Res.*, vol. 42, pp. 356–362, 2008.

[52] R. M. Richards, "Antimicrobial action of silver nitrate.," *Microbios*, vol. 31, pp. 83–91, 1981.

[53] P. Jena, S. Mohanty, R. Mallick, B. Jacob, and A. Sonawane, "Toxicity and antibacterial assessment of chitosan-coated silver nanoparticles on human pathogens and macrophage cells.," *Int. J. Nanomedicine*, vol. 7, pp. 1805–18, Jan. 2012.

[54] ATCC, "RAW 264.7 (ATCC ® TIB-71 ™) Product Sheet." American Type Culture Collection, 2013.

[55] N. C. Ammerman, M. Beier-Sexton, and A. F. Azad, "Growth and Maintenance of Vero Cell Lines," *Curr. Protoc. Microbiol.*, no. 11, pp. 1–10, 2008.

[56] T. Matsumura, V. Stollar, and R. W. Schlesinger, “Studies on the nature of dengue viruses,” *Virology*, vol. 46, no. 2, pp. 344–355, Nov. 1971.

[57] a T. Nahapetian, J. N. Thomas, and W. G. Thilly, “Optimization of environment for high density Vero cell culture: effect of dissolved oxygen and nutrient supply on cell growth and changes in metabolites.,” *J. Cell Sci.*, vol. 81, pp. 65–103, Mar. 1986.

[58] C.-C. Liu, S.-C. Lee, M. Butler, and S.-C. Wu, “High genetic stability of dengue virus propagated in MRC-5 cells as compared to the virus propagated in vero cells.,” *PLoS One*, vol. 3, no. 3, p. e1810, Jan. 2008.

[59] C. B. Anders, J. D. Baker, A. C. Stahler, A. J. Williams, J. N. Sisco, J. C. Trefry, D. P. Wooley, and I. E. Pavel Sizemore, “Tangential Flow Ultrafiltration: A ‘Green’ Method for the Size Selection and Concentration of Colloidal Silver Nanoparticles,” *J. Vis. Exp.*, no. October, pp. 1–9, 2012.

[60] M. I. Patel, R. Tuckerman, and Q. Dong, “A Pitfall of the 3-(4,5-dimethylthiazol-2-yl)-5(3-carboxymethonyphenol)-2-(4-sulfophenyl)-2H-tetrazolium (MTS) assay due to evaporation in wells on the edge of a 96 well plate.,” *Biotechnol. Lett.*, vol. 27, no. 11, pp. 805–8, Jun. 2005.

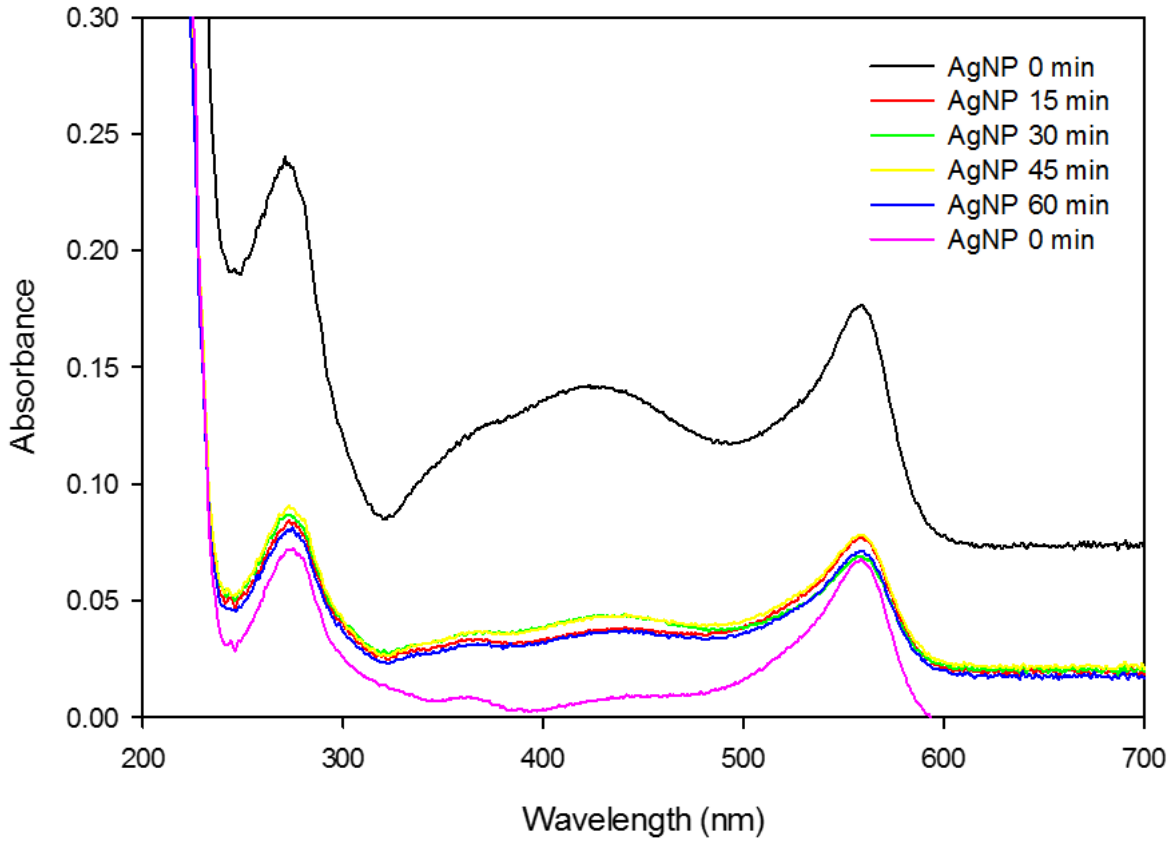

Supplemental Figure 1. AgNP (10 µg/mL) aggregate stability in DMEM-0.

Absorbance measured every 15 minutes for 1 hour. Lack of serum proteins in DMEM-0 caused rapid aggregation which remained stable for the 1 hour of measurements. Absorbance peak at 550 nm is phenol red.

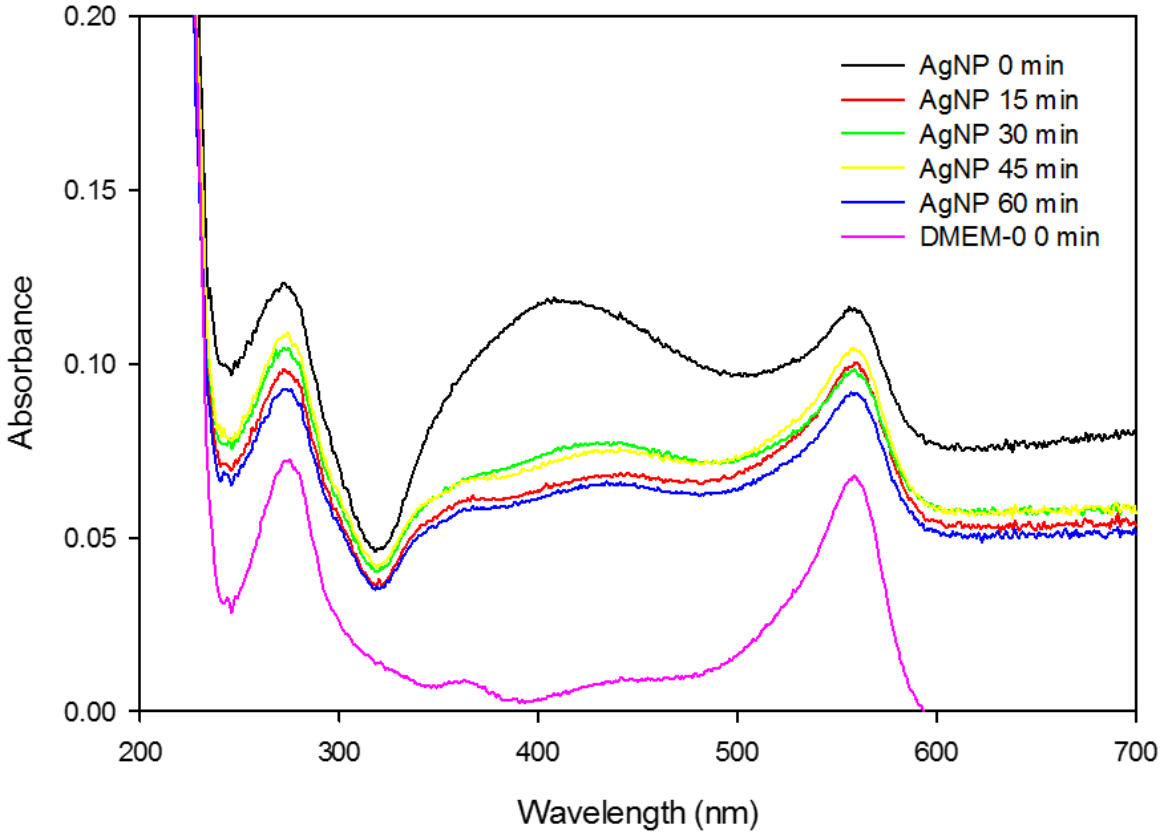

Supplemental Figure 2. AgNP (25 µg/mL) aggregate stability in DMEM-0.

Absorbance measured every 15 minutes for 1 hour. Lack of serum proteins in DMEM-0 caused rapid aggregation which remained stable for the 1 hour of measurements. Absorbance peak at 550 nm is phenol red.

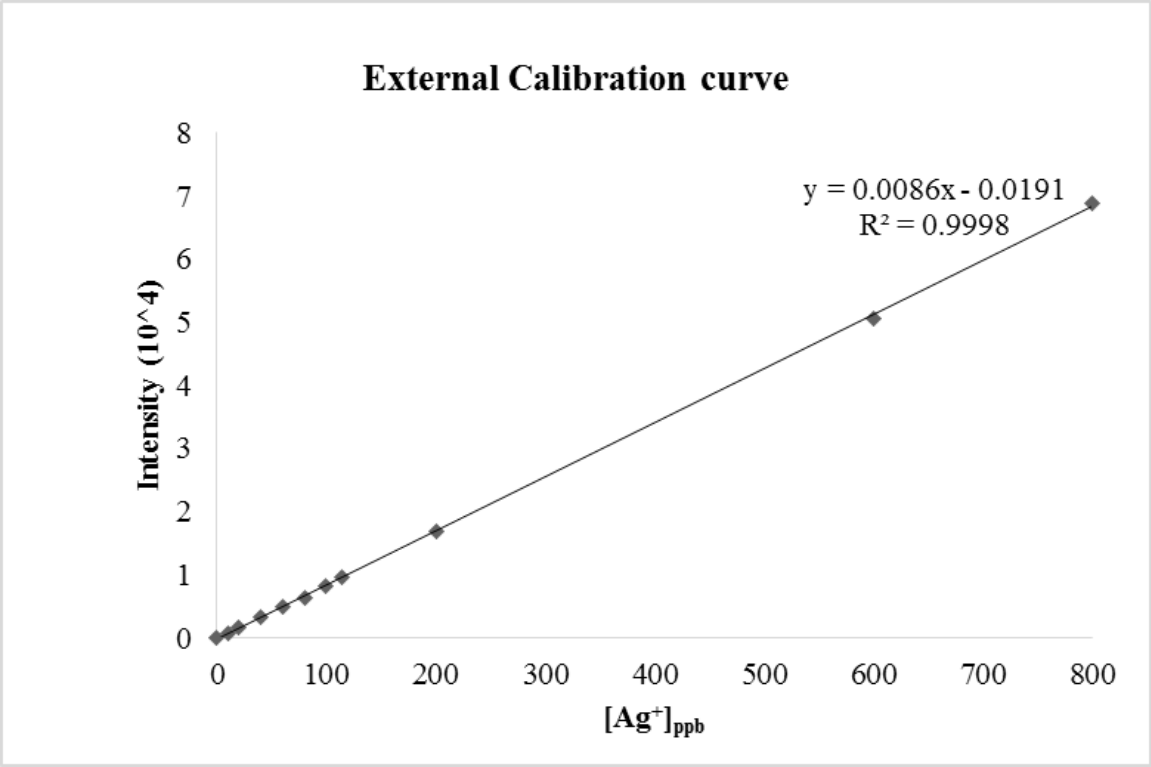

Supplemental Figure 3. ICP-OES Calibration curve